Searches for Dark Higgs Bosons at ATLAS

Changqiao Li
Max Planck Institute for Physics
(Werner Heisenberg Institute)

On behalf of the ATLAS collaboration

Roadmap of Dark Matter models for Run3, May 13-17, 2024

Two-Mediator DM (2MDM) model

- Simplified model for DM production at the LHC, extends spin-1 mediator models of LHC DM WG
    - Majorana DM (X) interacts with two different mediators:
        - Massive vector boson Z' and a dark Higgs s, is responsible for generating both DM and Z' mass

$$\mathcal{L}_\chi = \boxed{-g_q Z'^\mu \bar{q}\gamma_\mu q}$$

$$\mathcal{L}_\chi = \boxed{-\frac{1}{2} g_\chi Z'^\mu \bar{\chi}\gamma^5\gamma_\mu\chi} - \boxed{g_\chi \frac{m_\chi}{m_{Z'}} s\bar{\chi}\chi} + \boxed{2\, g_\chi\, Z'^\mu Z'_\mu \left(g_\chi\, s^2 + m_{Z'} s\right)}$$

- Parameters and their recommended value from LHC DM WG

Particle Masses		**Couling Constants**	
Majorana DM mass	m_χ = 200 GeV	Dark-sector coupling	g_χ = 1.0
Z' mass	$m_{Z'}$	Quark-Z' coupling	g_q = 0.25
Dark Higgs mass	m_s	Mixing angle with SM Higgs	θ = 0.01

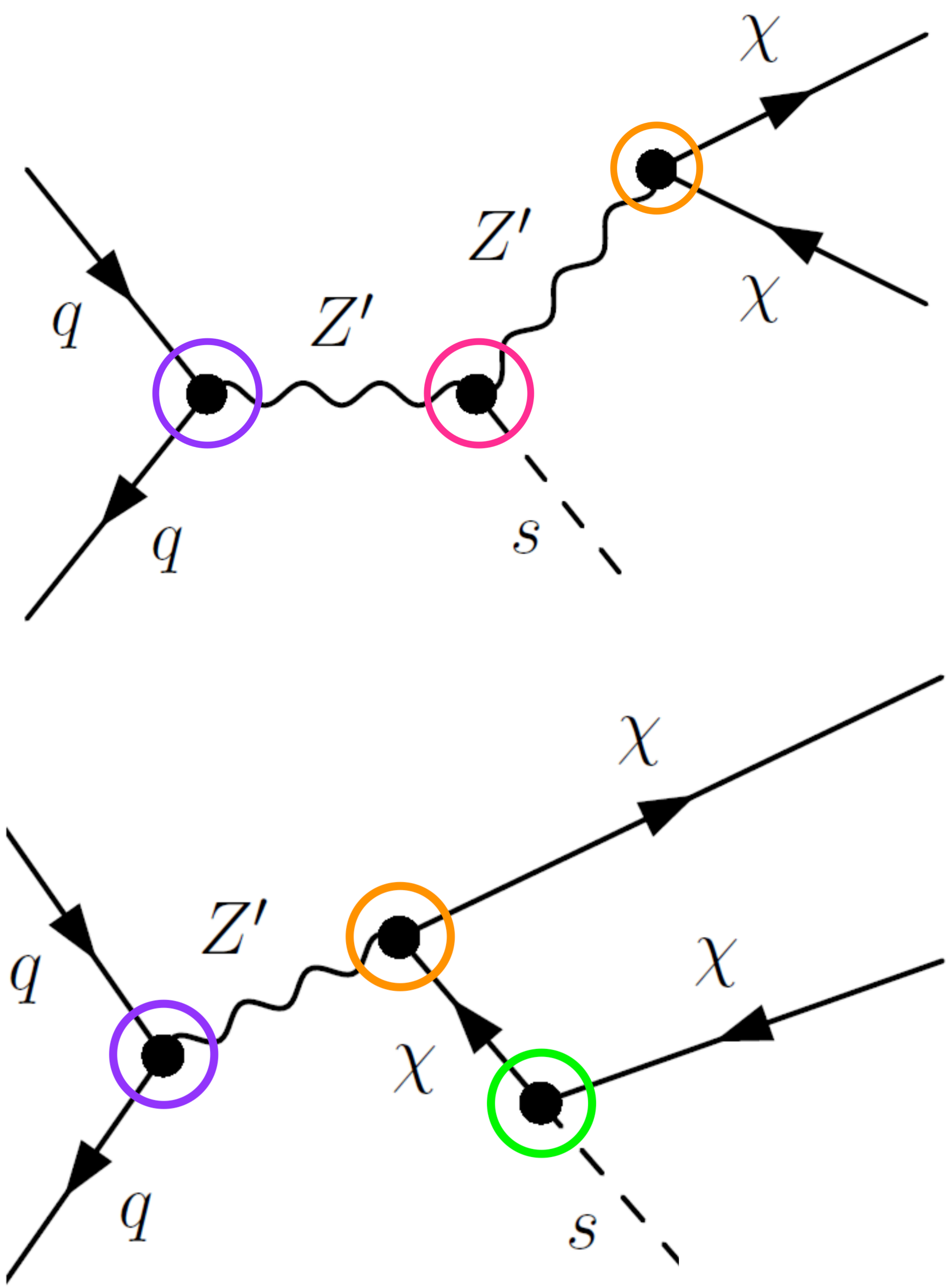

Various final states Targeted

Non-Zero θ → unstable s and decays into SM states

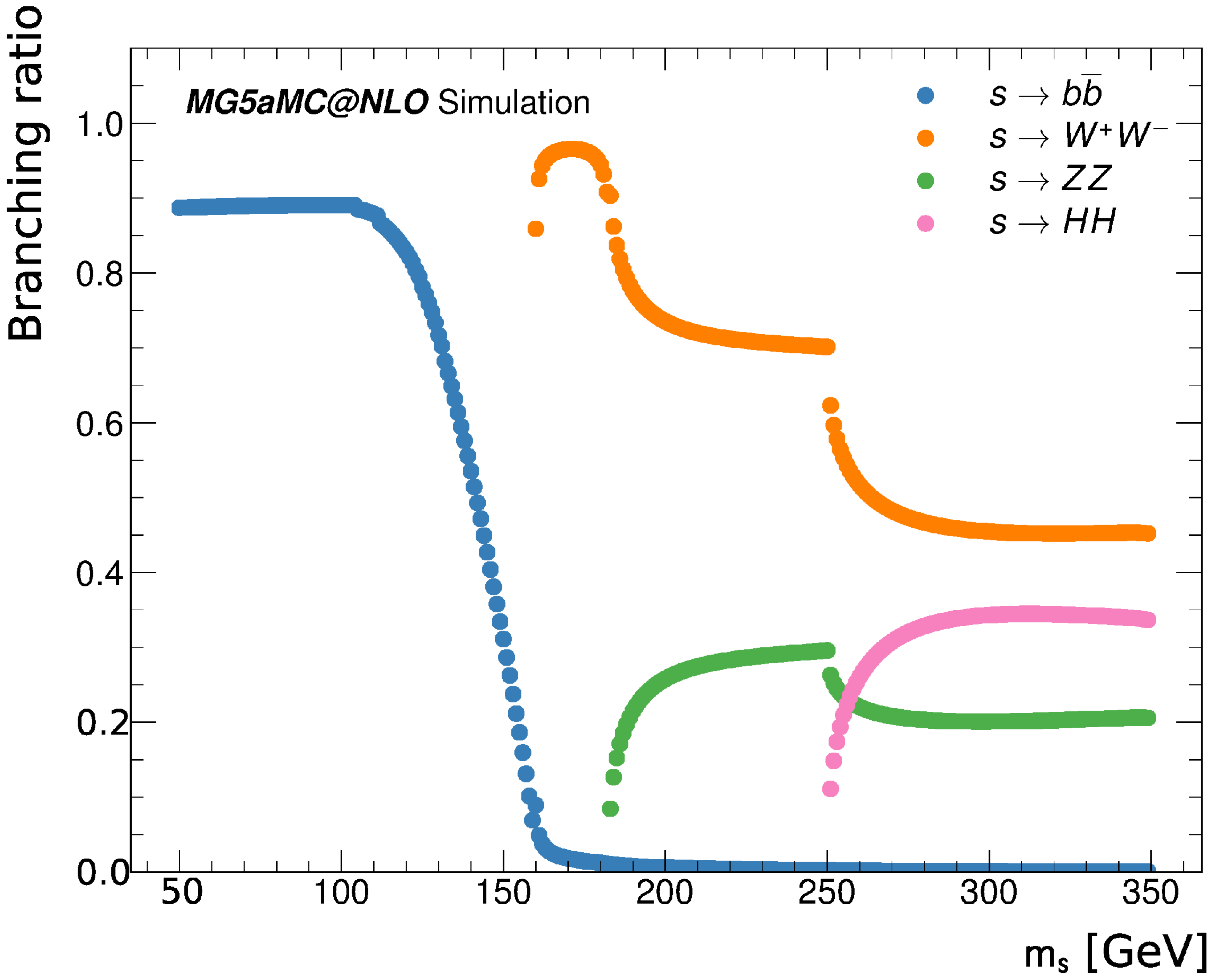

m_S > 150 GeV

Dark Higgs s(VV) hadronic analysis, denoted as *monoSVV had.*

- Final states: E_T^{miss} + VV(qqqq)
- Phys. Rev. Lett. 126 (2021) 121802

Dark Higgs s(WW) semileptonic analysis, denoted as *monoSWW semilep.*

- Final states: E_T^{miss} + WW(lvqq)
- Higher cross section than fully-leptonic
- Cleaner signature than fully-hadronic
- JHEP 07 (2023) 116

$m_S \leq$ 150 GeV

Dark Higgs s(bb) analysis, denoted *monoSbb*

- Final states: E_T^{miss} + bb
- Dominates in low m_S
- ATLAS-CONF-2024-004

Reconstruction of the s decay

$m_s > 150$ GeV

monoSVV had.

Merged

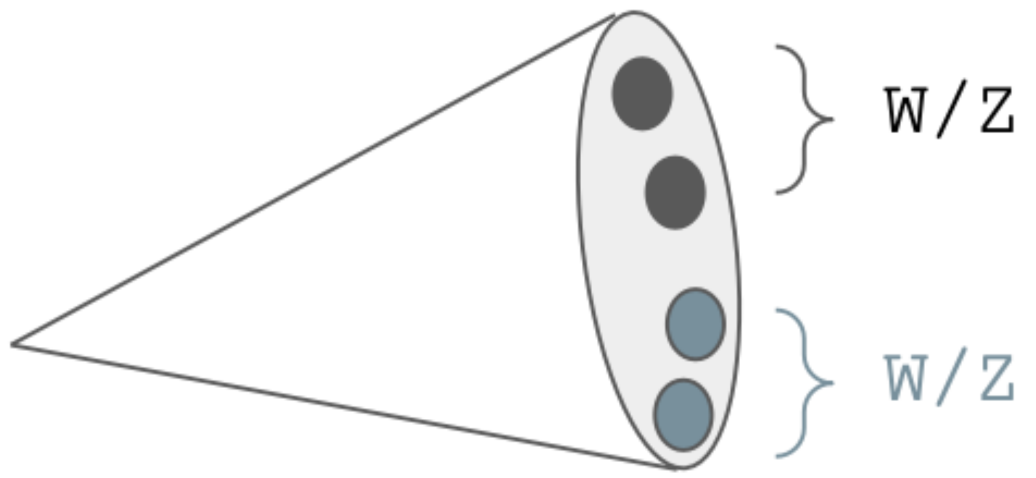

Intermediate

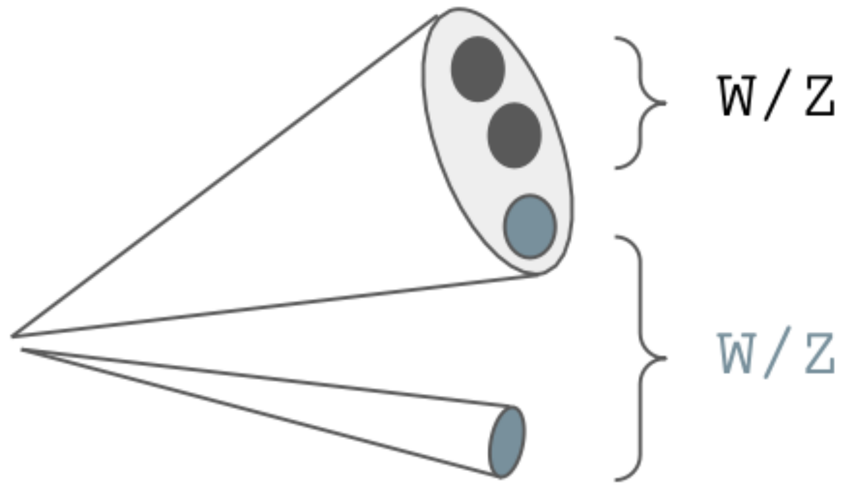

monoSWW semilep.

Merged

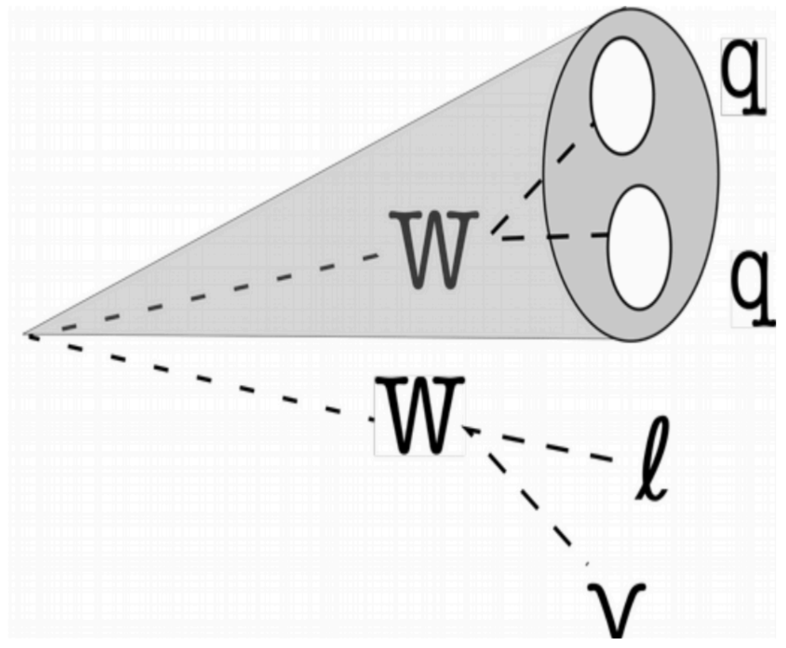

Resolved

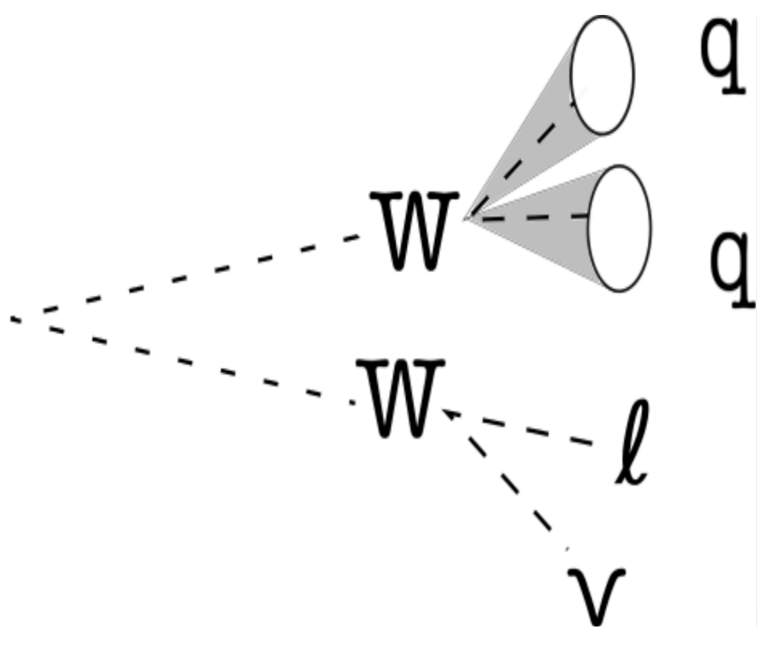

$m_s \leq 150$ GeV

monoSbb

Merged

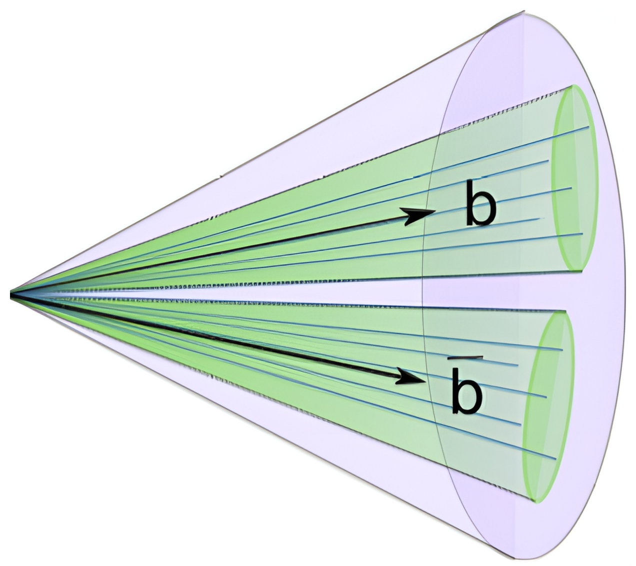

Resolved

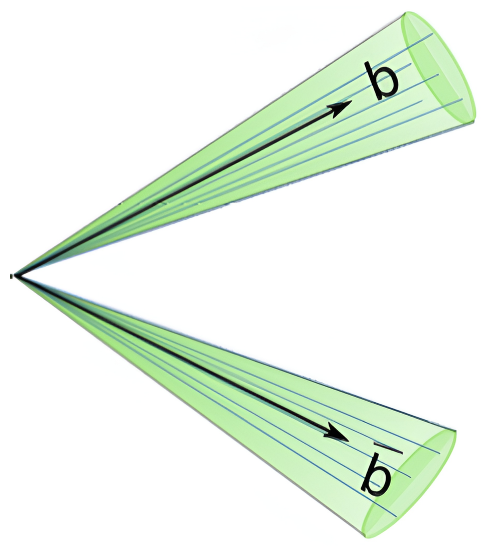

In all three analyses, Merged SR dominates sensitivity

Reconstruction techniques used in Merged / Intermediate regions	
monoSbb	*Reclustered large-R* jets (allows for exploring the low m_s)+ *Xbb* tagger
monoSVV had. / monoSWW semilep.	*Reclustered* + *track assisted large-R* jets + the cuts on the substructure variables

Reclustering and Track Assisted large-R jets

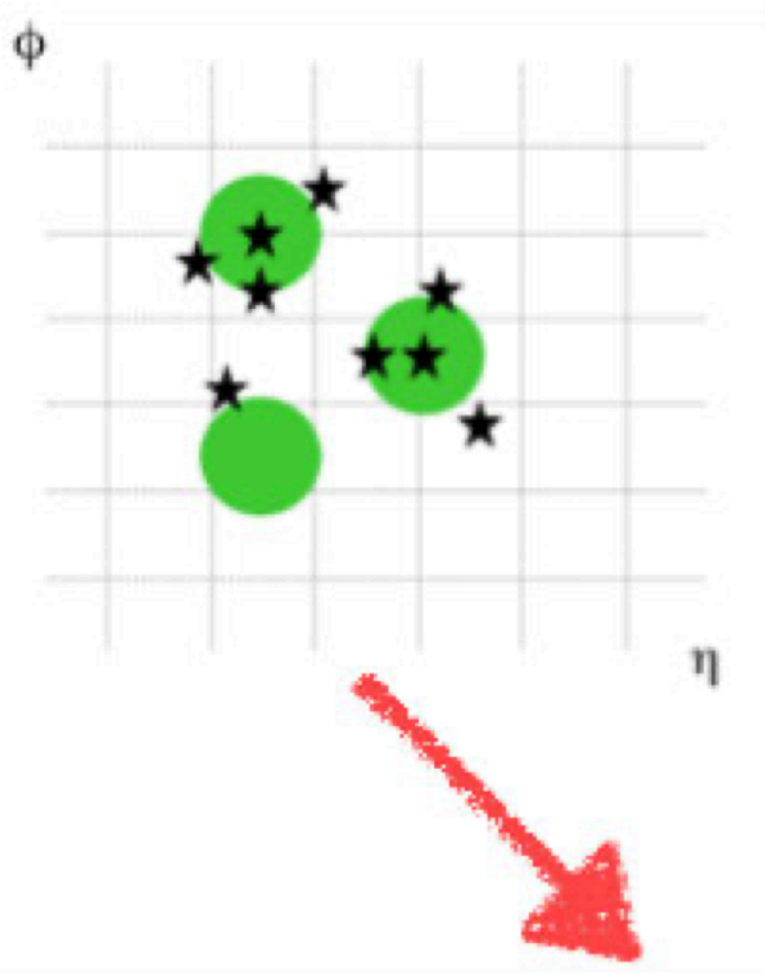

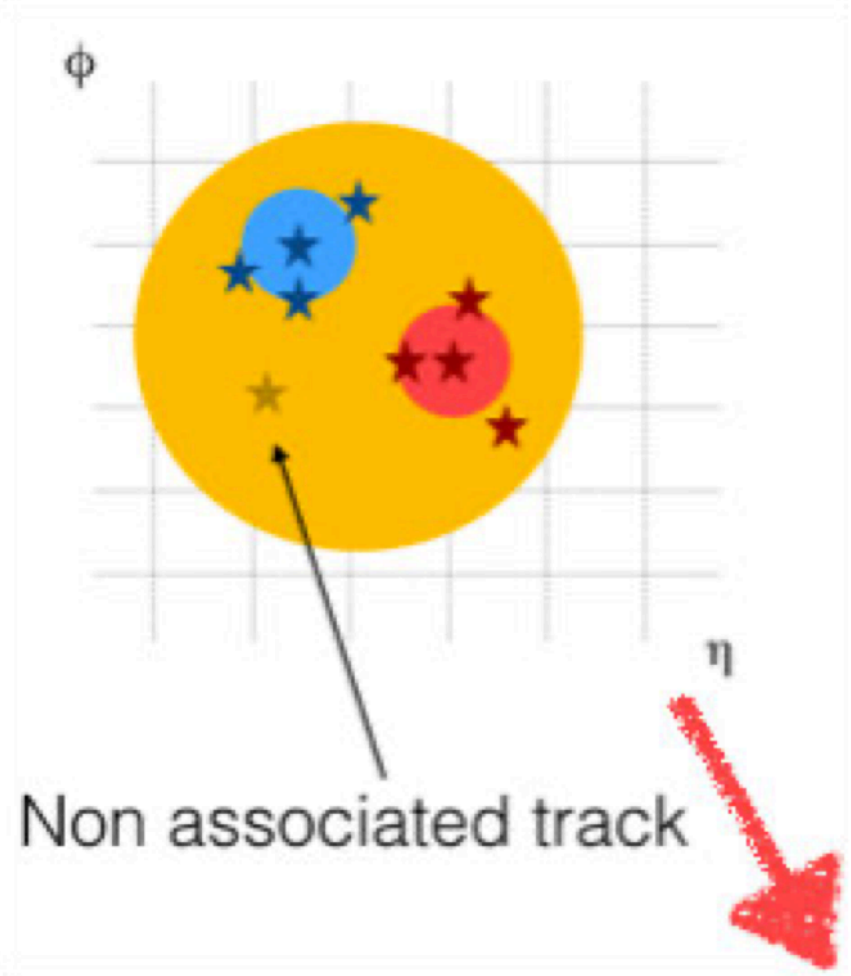

Use excellent angular resolution of the ATLAS tracker system

$$p_{\mathrm{T}}^{\mathrm{track,new}} = p_{\mathrm{T}}^{\mathrm{track,old}} \times \frac{p_{\mathrm{T}}^{j}}{\sum_{i \in j} p_{\mathrm{T}}^{i}}$$

where the index i runs over all tracks matched to subjet j

Track Assisted Reclustering

Callibrated small-radius jets → Recluster input jets to trimmed large-radius jets → Match tracks to constituent small-radius jets → Rescale tracks to p_T of the matched small-radius jets → Calculate substructure from tracks

Tracks ↑ (into "Match tracks to constituent small-radius jets")

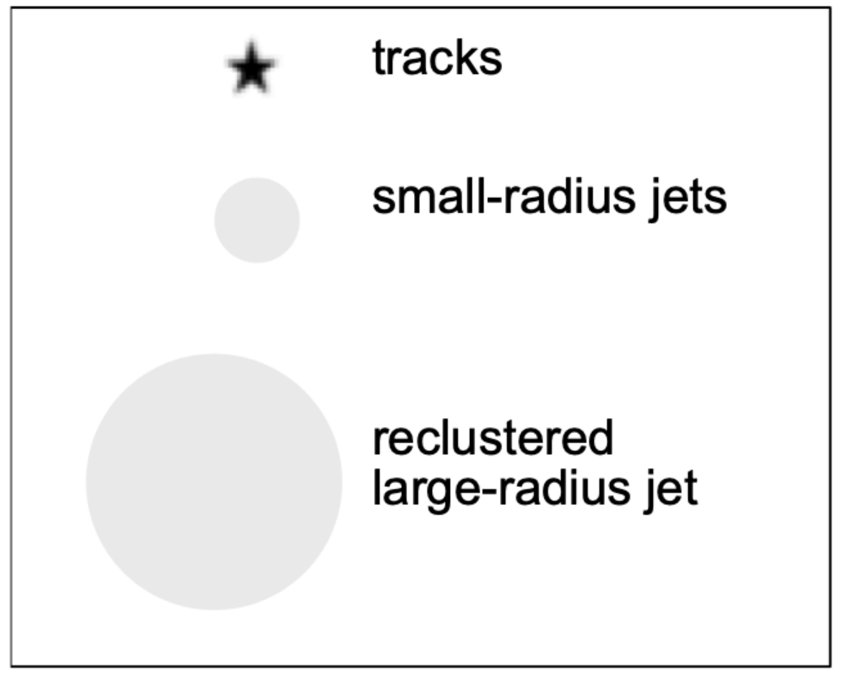

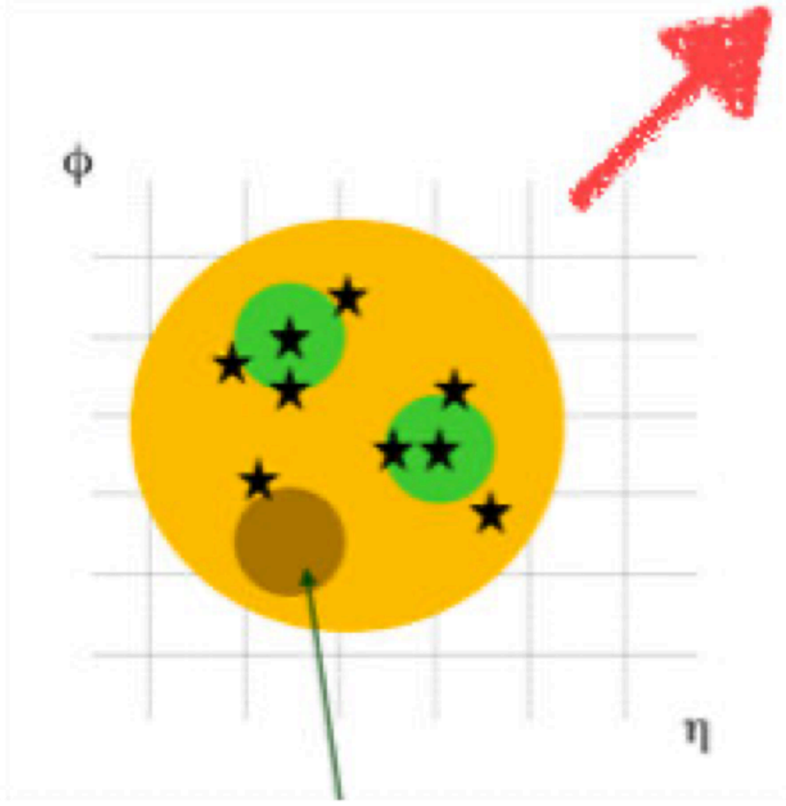

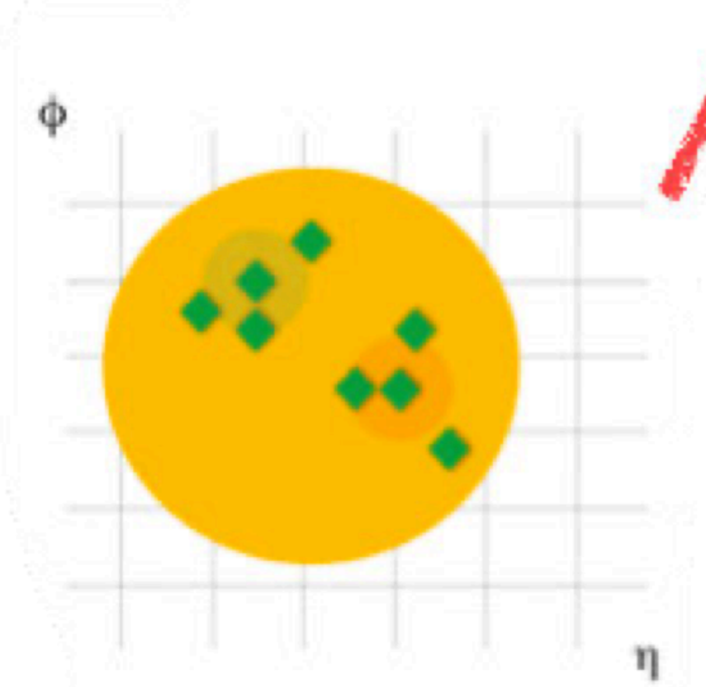

credit to monoSVV team

monoSVV had.
Analysis

Overview

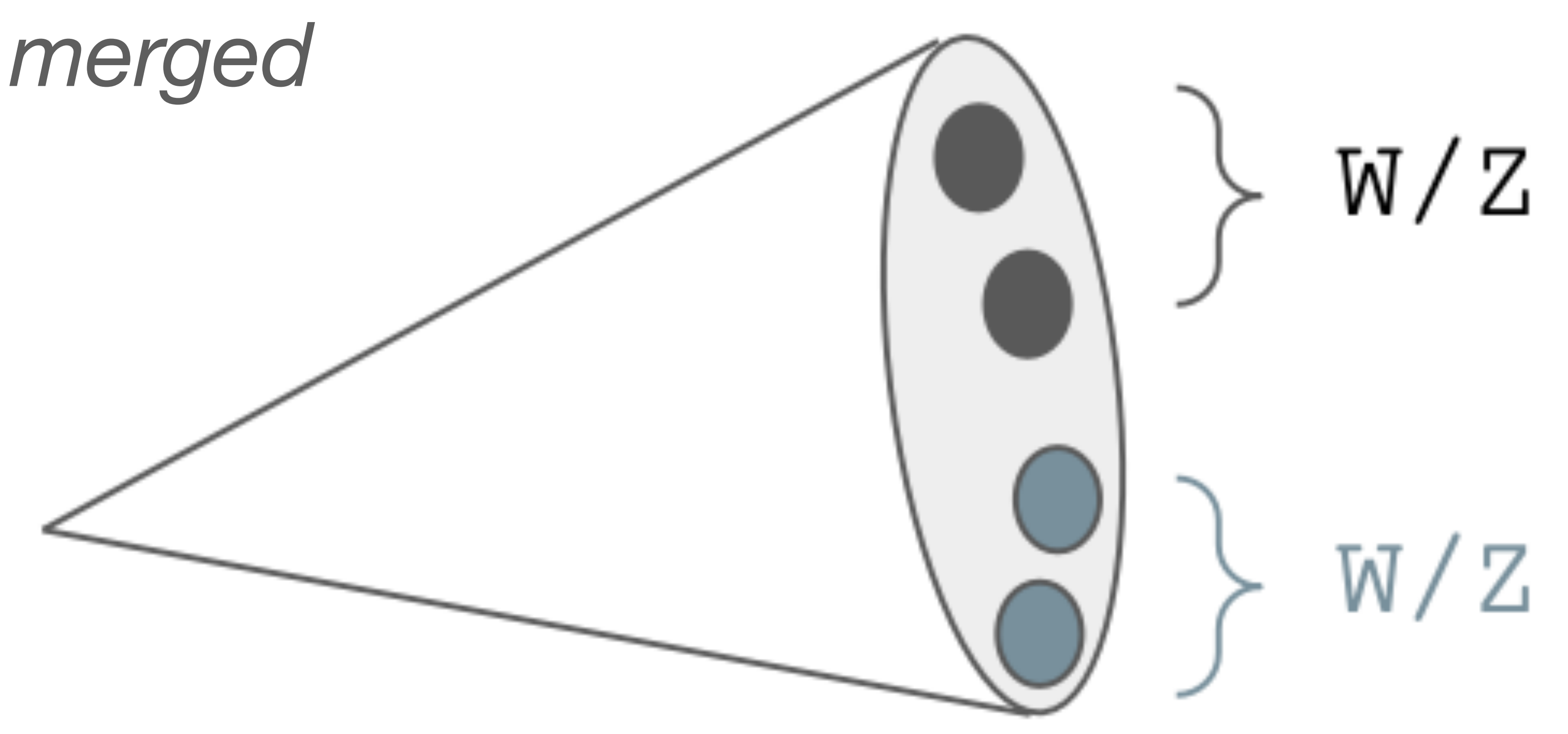

R=0.8 TAR jet with highest pt with τ_{42}<0.3 and τ_{43}<0.6 $m_{VV} = m_{TAR}$

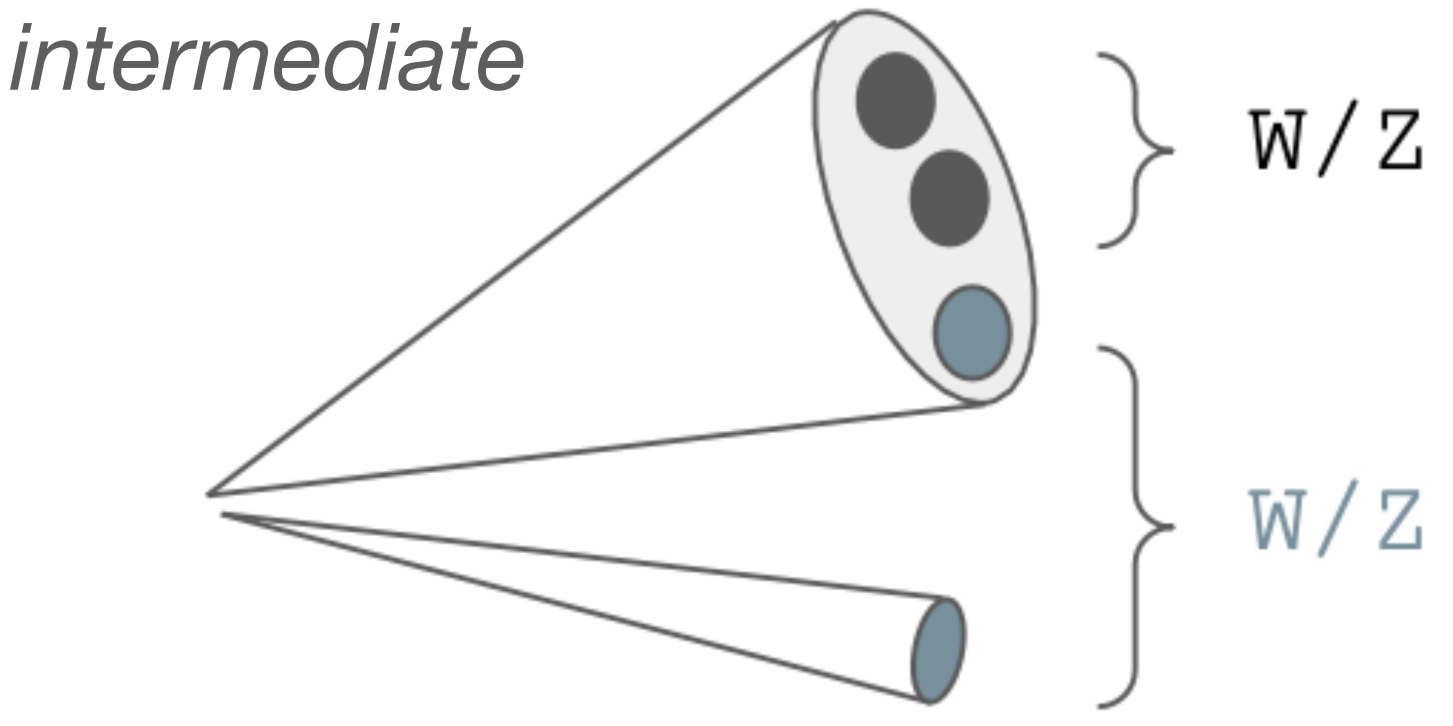

R=0.8 TAR jet with 1-2 small-radius jets $m_{VV} = m_{TAR+COMB}$

✖

0 lepton	1 μ	2 lepton
signal region	W+jets control region	Z+jets control region
E_T^{miss} bins	E_T^{miss} proxy = $(E^{miss} + p^{\mu})_T$ bins	E_T^{miss} proxy = $p_T(ll)$ bins

- E_T^{miss} triggers used in 0 lepton and 1 μ channel, combination of single lepton triggers in 2 lepton channel
- N(small-R jets) ≥ 2, dedicated # of lepton for each channel, E_T^{miss}(or E_T^{miss} proxy) > 200 GeV
- anti-QCD cuts, tau veto, b-tag veto

Reconstructed m_{VV} in CR

E_T^{miss}	200 - 300 GeV	300 - 500 GeV	> 500 GeV
merged	not considered	prioritized	prioritized
intermediate	prioritized	not prioritized	not prioritized

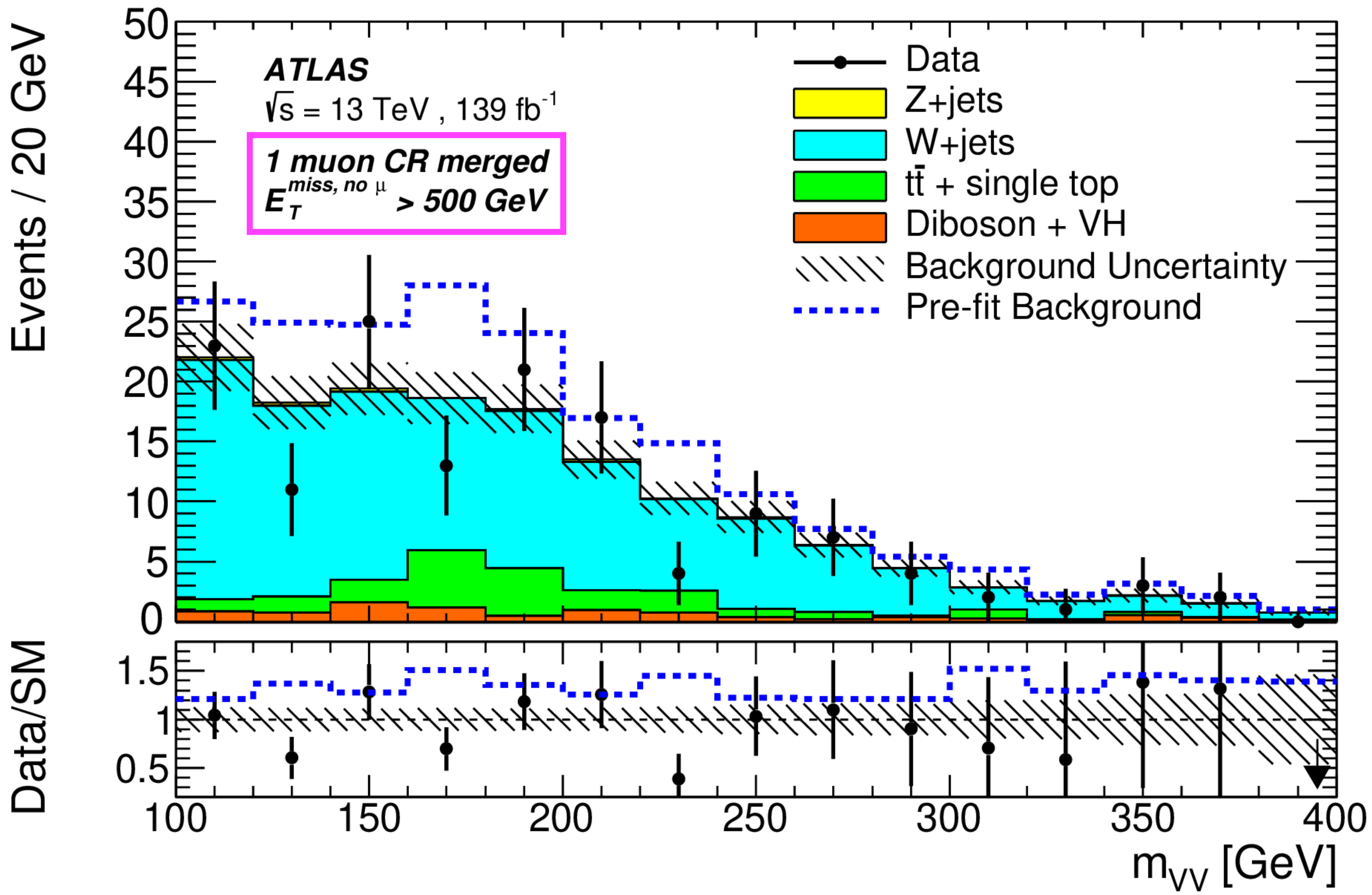

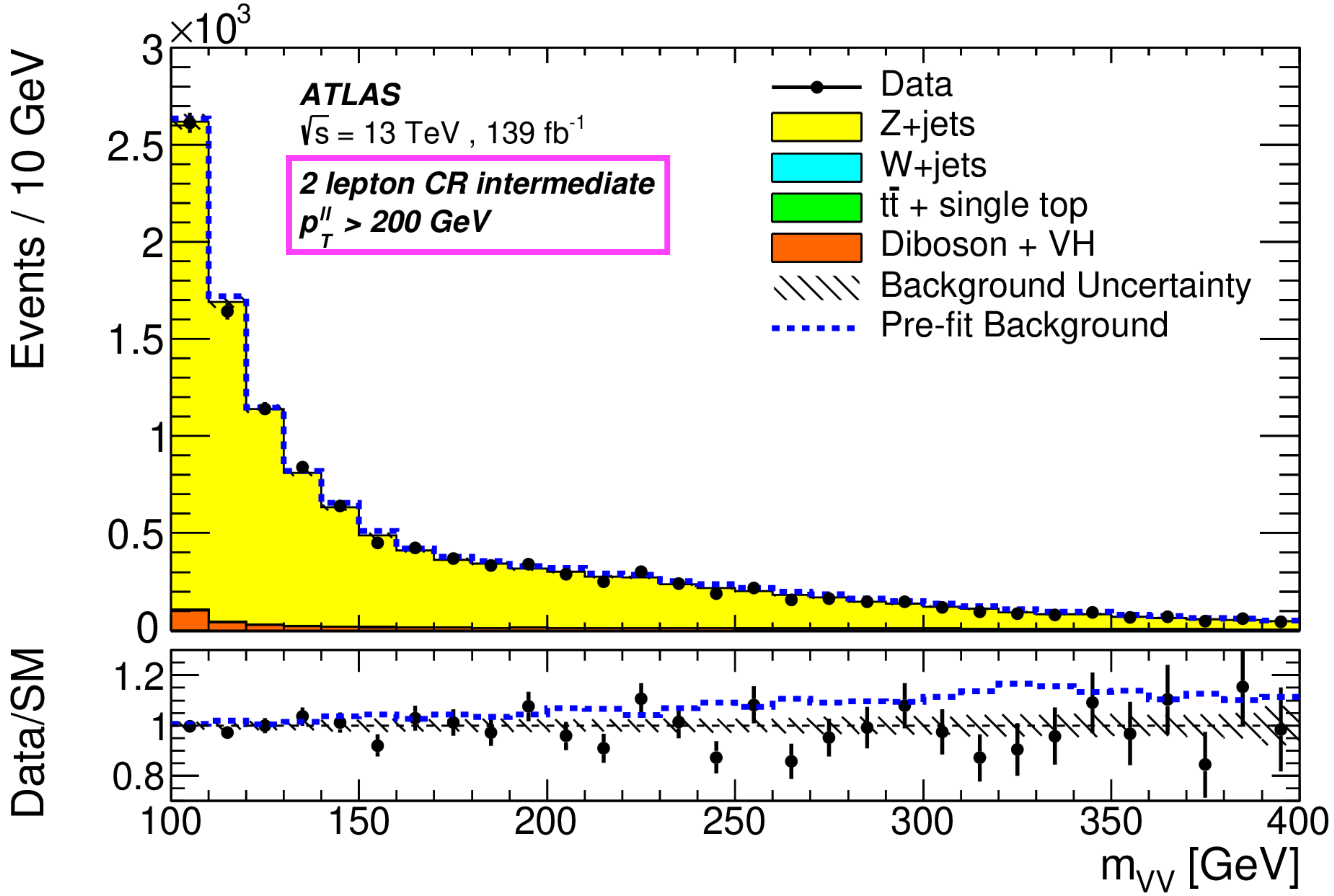

A good modelling of the mVV observed, only yield information in CRs used in fit, shape not

Reconstructed m_{VV} in SR

E_T^{miss}	200 - 300 GeV	300 - 500 GeV	> 500 GeV
merged	not considered	prioritized	prioritized
intermediate	prioritized	not prioritized	not prioritized

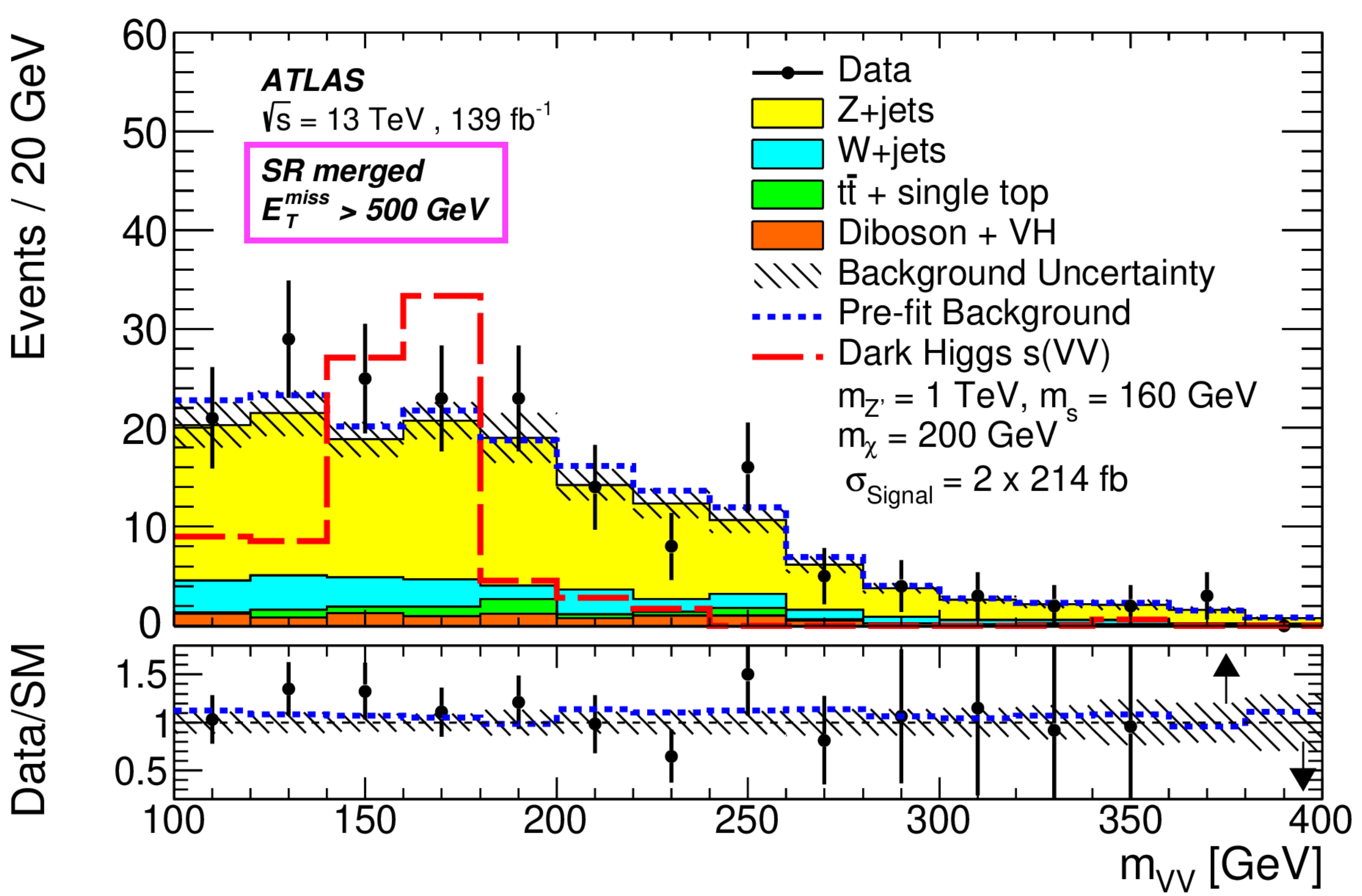

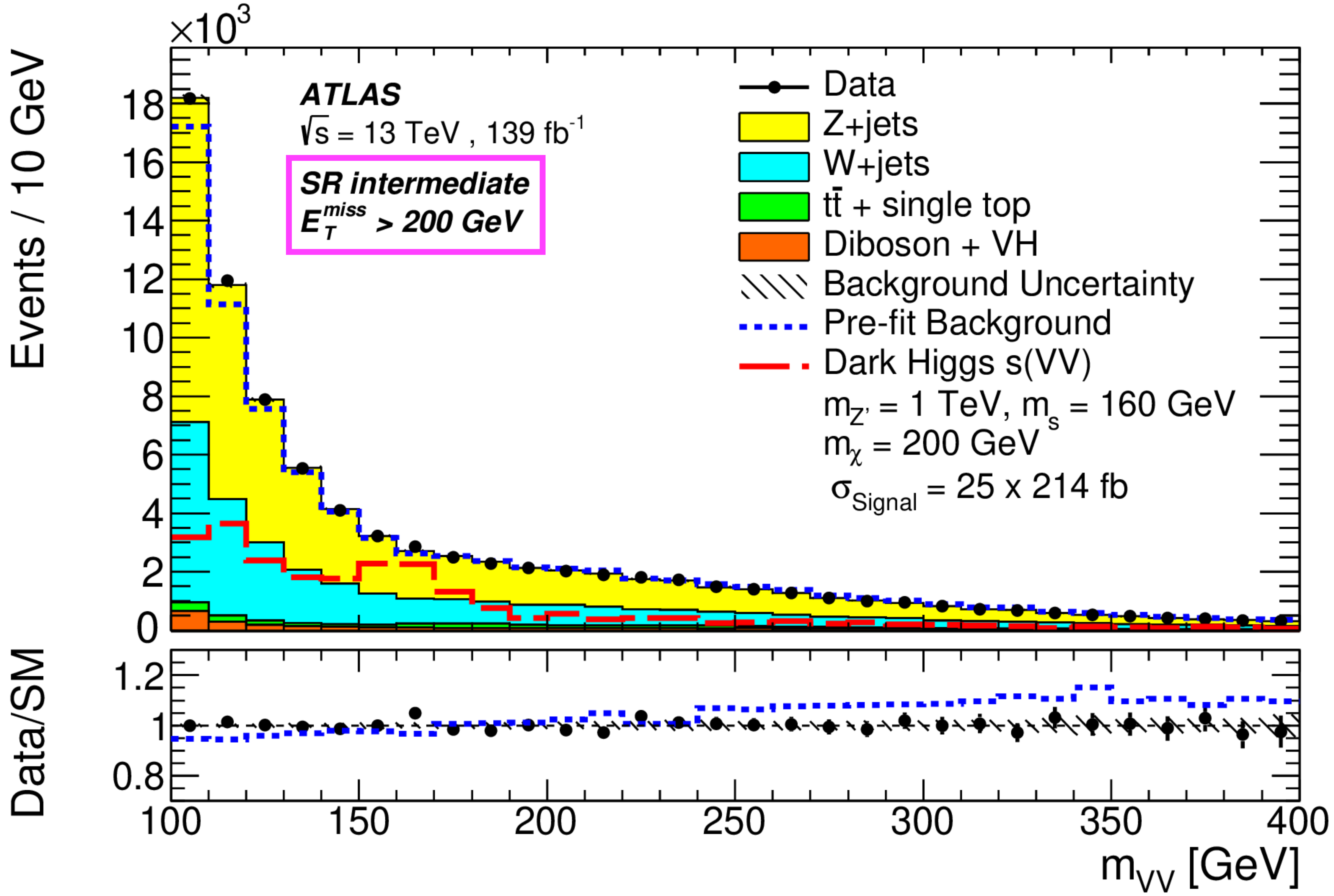

fit on m_{VV} shape in the SRs

Dominant Sources of Uncertainty

Source of uncertainty	Uncertainty [%] (a)	(b)	(c)
Signal modeling	11	10	10
W+jets modeling	9	21	14
Z+jets modeling	7	12	13
MC statistics	11	14	23
Jet energy scale	8	17	24
Jet energy resolution	11	18	15
Lepton reconstruction	8	9	5
Track reconstruction	6	7	5
Systematic uncertainty	30	42	55
Statistical uncertainty	16	25	50
Total uncertainty	34	49	74

3 selected signals

	$m_{Z'}$ [TeV]	m_s [GeV]
a	1	160
b	1	235
c	1	310

Strongest impact on theory predicted signal strength from:

- W/Z+jets modelling
- Jet systematics
- signal modelling

systematics dominated

Limit Contours in $m_{Z'}$-m_S-plane

- TAR jet can improve the sensitivity up to 2.5 compared to conventional large-R jet

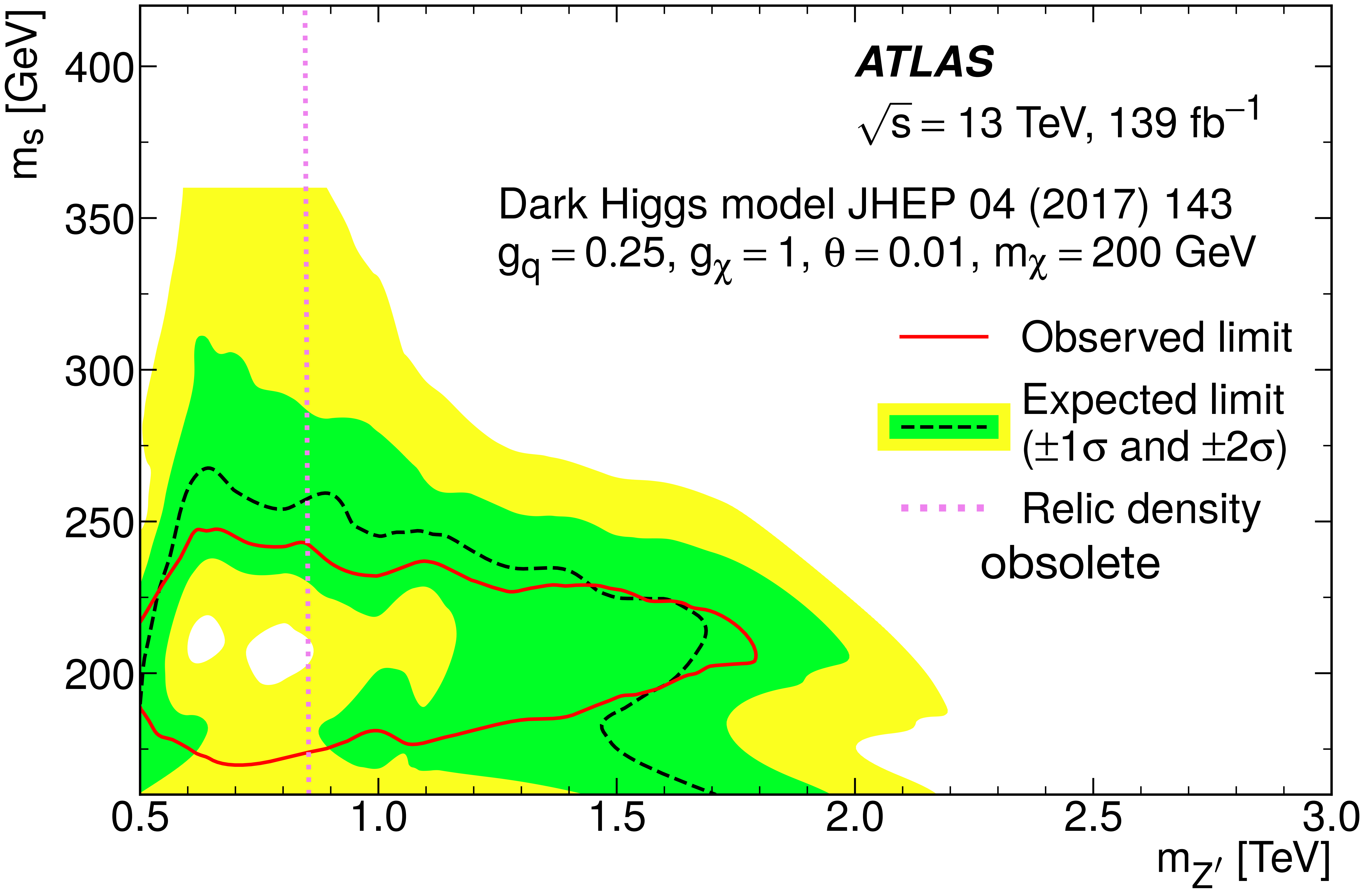

monoSWW semilep. Analysis

Overview

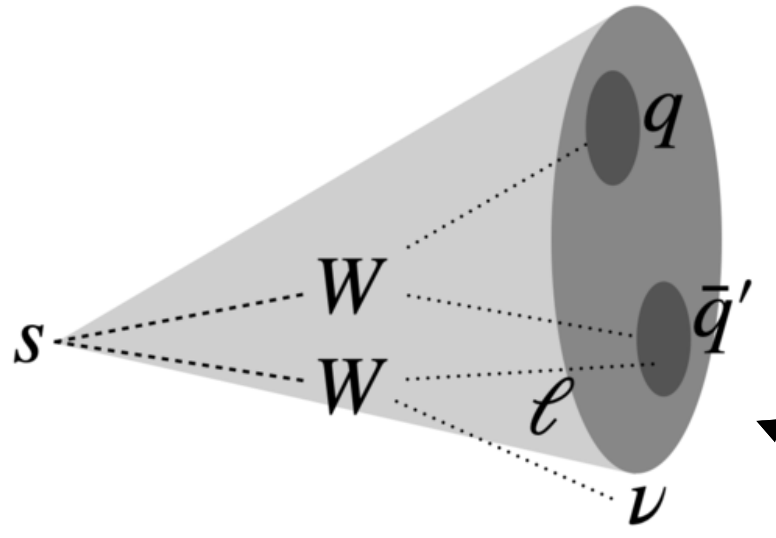

merged

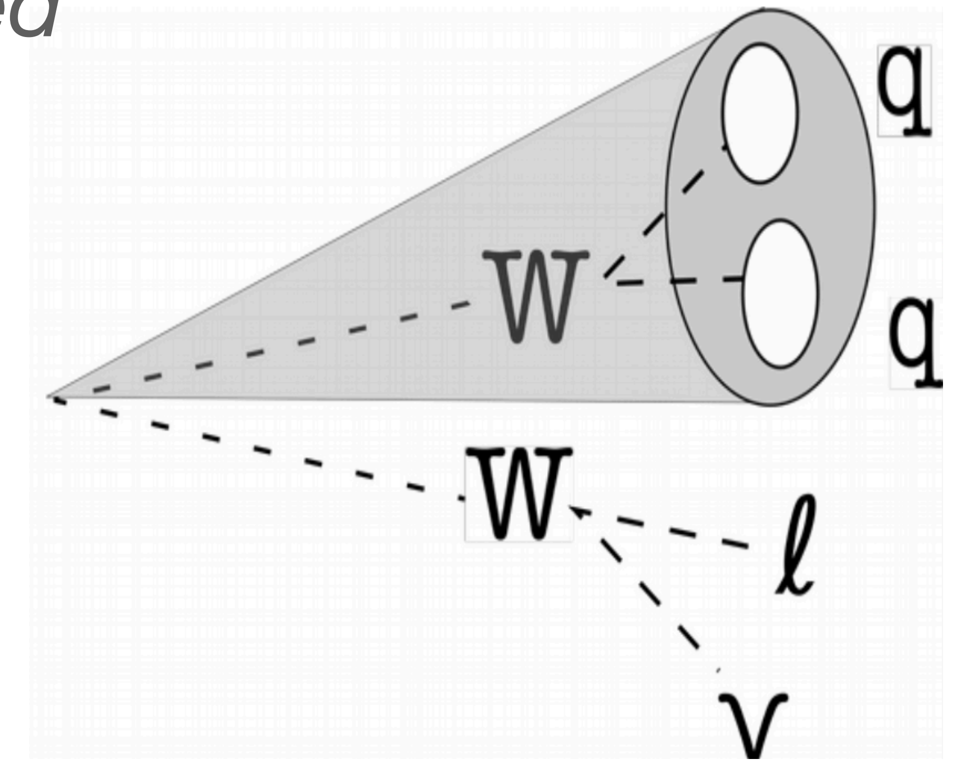

W_{had} candidate: R=1.0 TAR jet

lepton disentanglement and $D_2^{\beta=1} < 1.1$

resolved

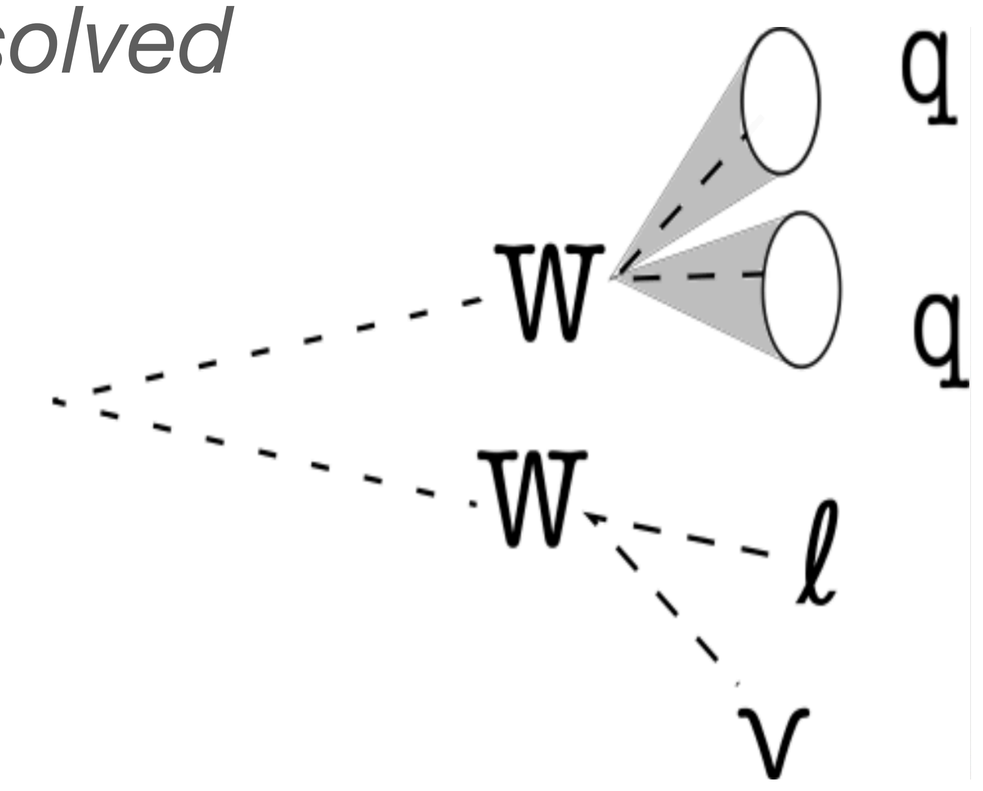

W_{had} candidate: 2 R=0.4 jets with

m(j,j) closest to W mass

×

	SR	W+jets CR	ttbar CR
$N_{b\text{-jet}}$	0	0	≥ 2
$\Delta R(W_{can.}, \text{lep})$	<1.2	>1.8	<1.2

- passed E_T^{miss} trigger or single muon trigger, N(lep) = 1, high E_T^{miss} and high $m_T(\text{lep}, E_T^{miss})$
- E_T^{miss} significance cuts, window cut on $m_{Wcand.}$
- Recycling strategy: Only consider events for the resolved category if they fail the merged criteria

Analytical solution of s→WW→qqlv system

- 3 invisible (neutrino + 2 DM) particle in the decay products → direct dark-Higgs reconstruction impossible
- Used a rotated frame of reference with lepton along Z-axis and W_{had} in X-Z plane.
- Find minimum m_s (m_s^{min}) consistent with W_{had} and lepton momenta and m_W constraint. details in backup

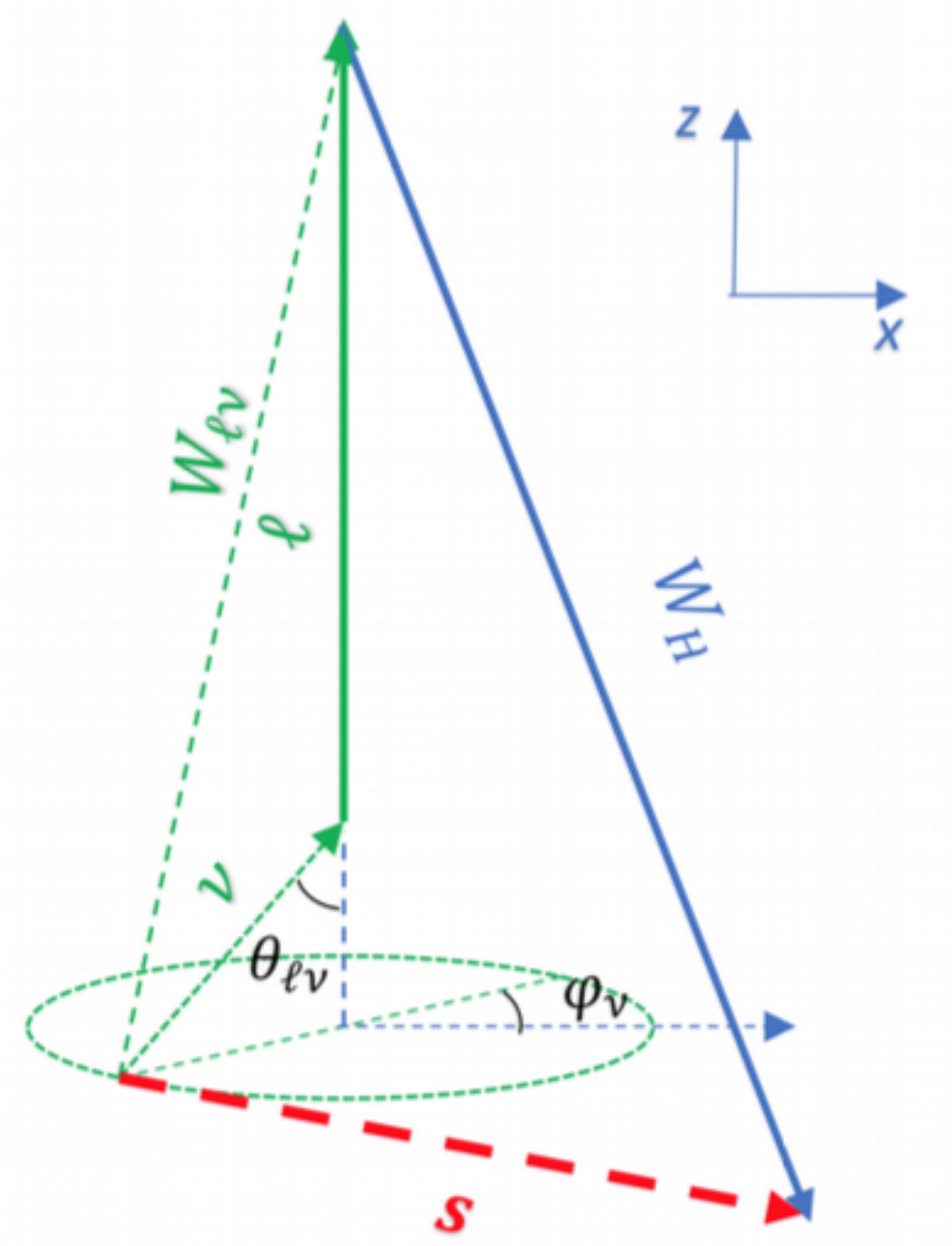

credit to monoSWW team

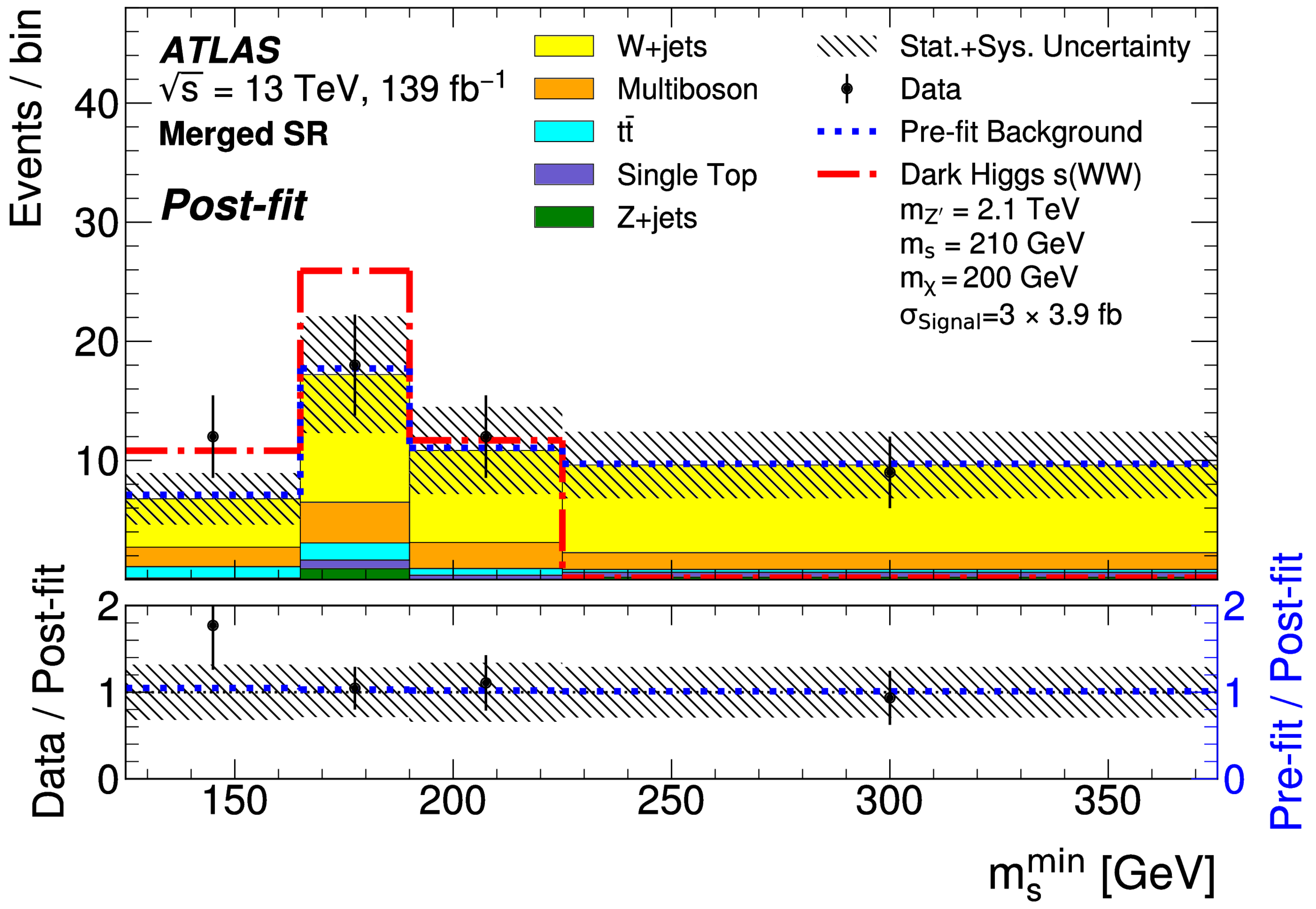

fit on m_s^{min} shape in the SRs + yield in CRs simultaneously

Dominant Sources of Uncertainty

Source of uncertainty	Uncertainty [%]		
	(2100, 210)	(1000, 140)	(1000, 360)
W+jets modelling	4	5	2
Diboson modelling	5	4	1
$t\bar{t}$ modelling	7	4	1
Single top modelling	9	5	11
Signal modelling	1	3	0
Statistical uncertainty of MC	26	15	29
$R = 0.4$ jet energy scale	11	12	14
$R = 0.4$ jet energy resolution	9	4	7
$R = 0.2$ jet energy scale	9	9	14
$R = 0.2$ jet energy resolution	13	10	16
$E_{\mathrm{T}}^{\mathrm{miss}}$	7	1	7
Track reconstruction	5	2	2
Lepton reconstruction	2	3	1
Systematic uncertainty	38	28	40
Statistical uncertainty of data	38	32	37
Total uncertainty	53	43	55

($m_{Z'}$, m_s)

Strongest impact on fitted signal strength from:

- MC statistics (mainly W+jets)
- Jet uncertainties

systematic uncertainty (incl. MC statistics) is comparable to statistical uncertainty

Limit Contours in $m_{Z'}$-m_S-plane

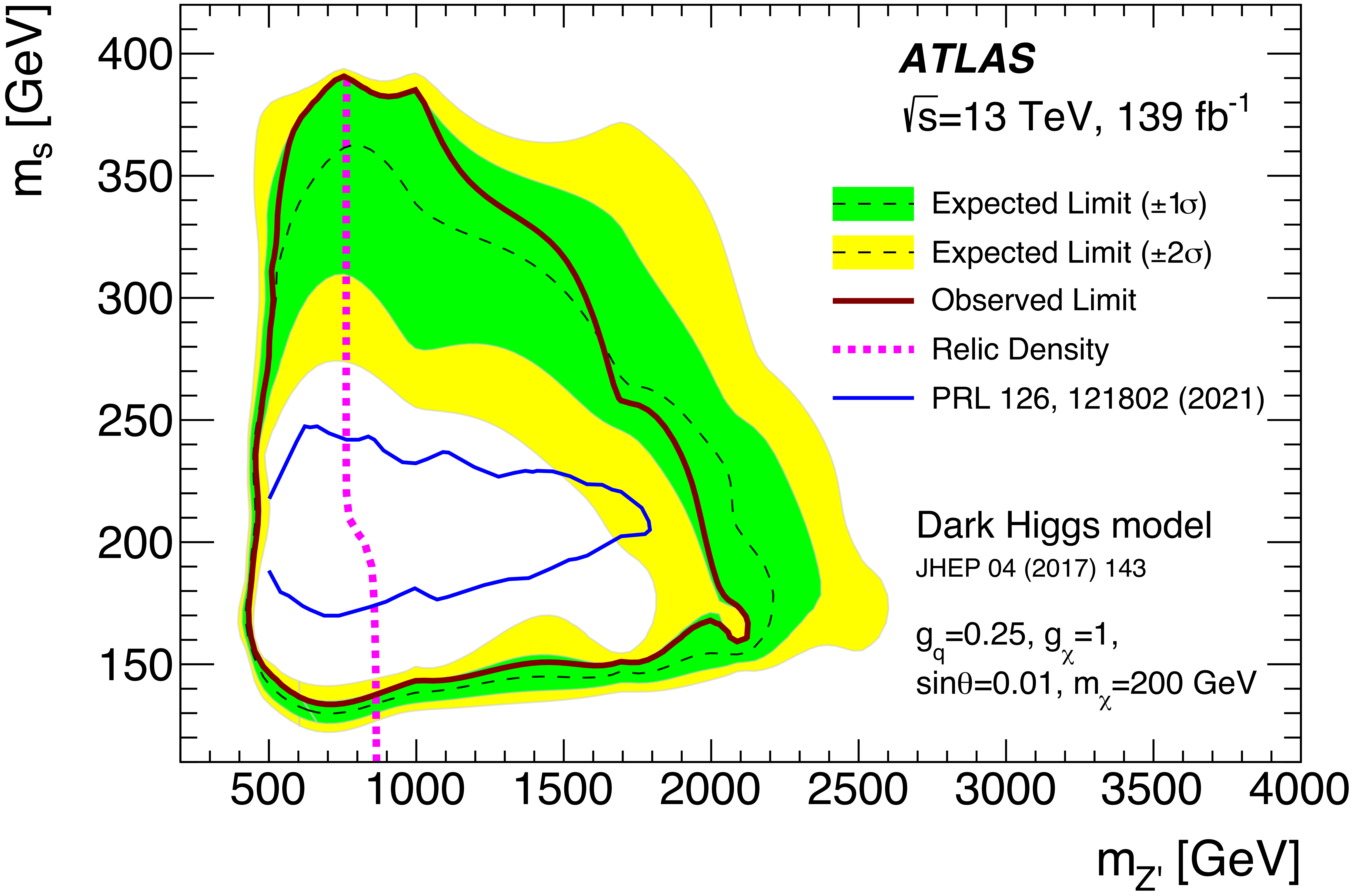

monoSbb Analysis

Overview

merged

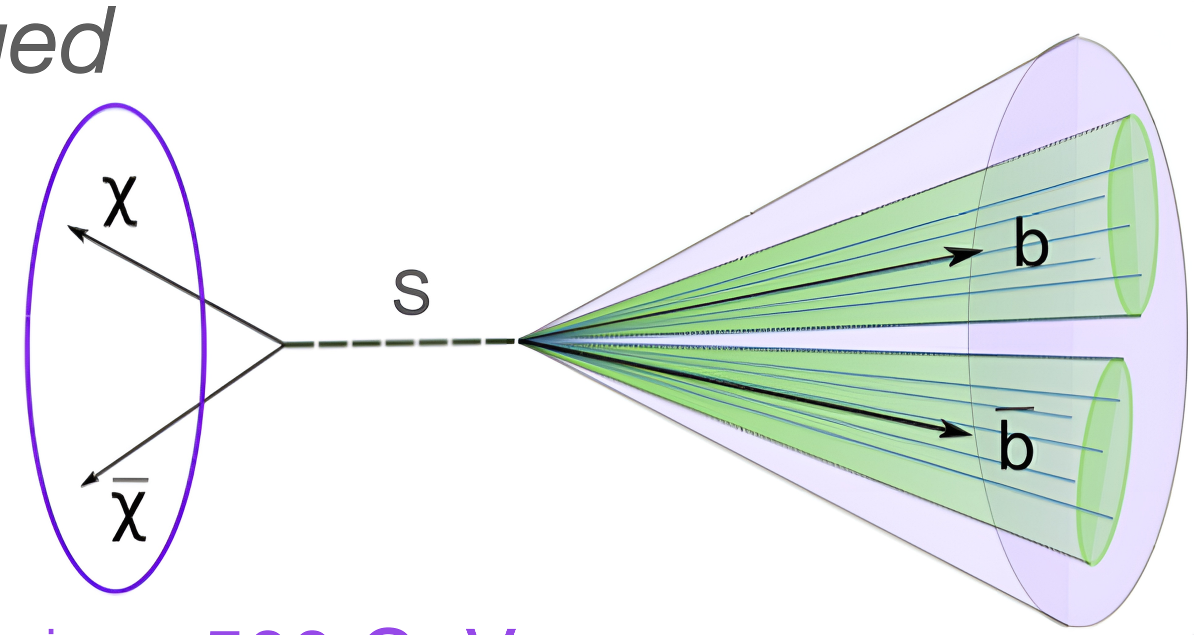

$E_T^{miss} > 500$ GeV

1 Reclustering R=1.0 jet (RC jet)

tagged by Xbb tagger or by 2 associated

VR trkjet DL1r tagger, $m_s = m_J$ (RC jet mass)

resolved

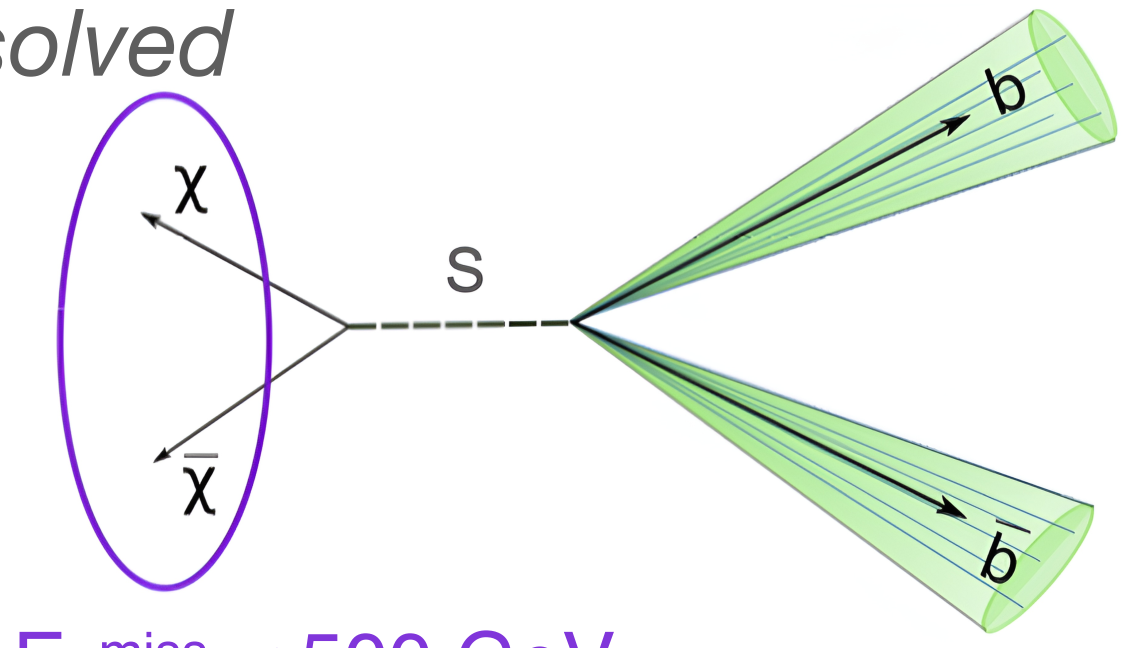

$150 < E_T^{miss} < 500$ GeV

2 R=0.4 PFlow jets

tagged by DL1r tagger, $m_s = m_{bb}$

✖

0 lepton	1 μ	2 lepton
signal region	W+jets + ttbar control region	Z+jets control region
E_T^{miss} bins	E_T^{miss} proxy = $(E^{miss} + p^{\mu})_T$ bins	E_T^{miss} proxy = $p_T(ll)$ bins

- E_T^{miss} triggers used in 0 lepton and 1 μ channel, combination of single lepton triggers in 2 lepton channel
- dedicated # of lepton for each channel, E_T^{miss} and Sbb recoil, boosted decay with 2m/pT < 0.6 for RC jet
- anti-QCD cuts, tau veto, b-tag veto outside RC jet

Reconstruction of the s→bb

merged

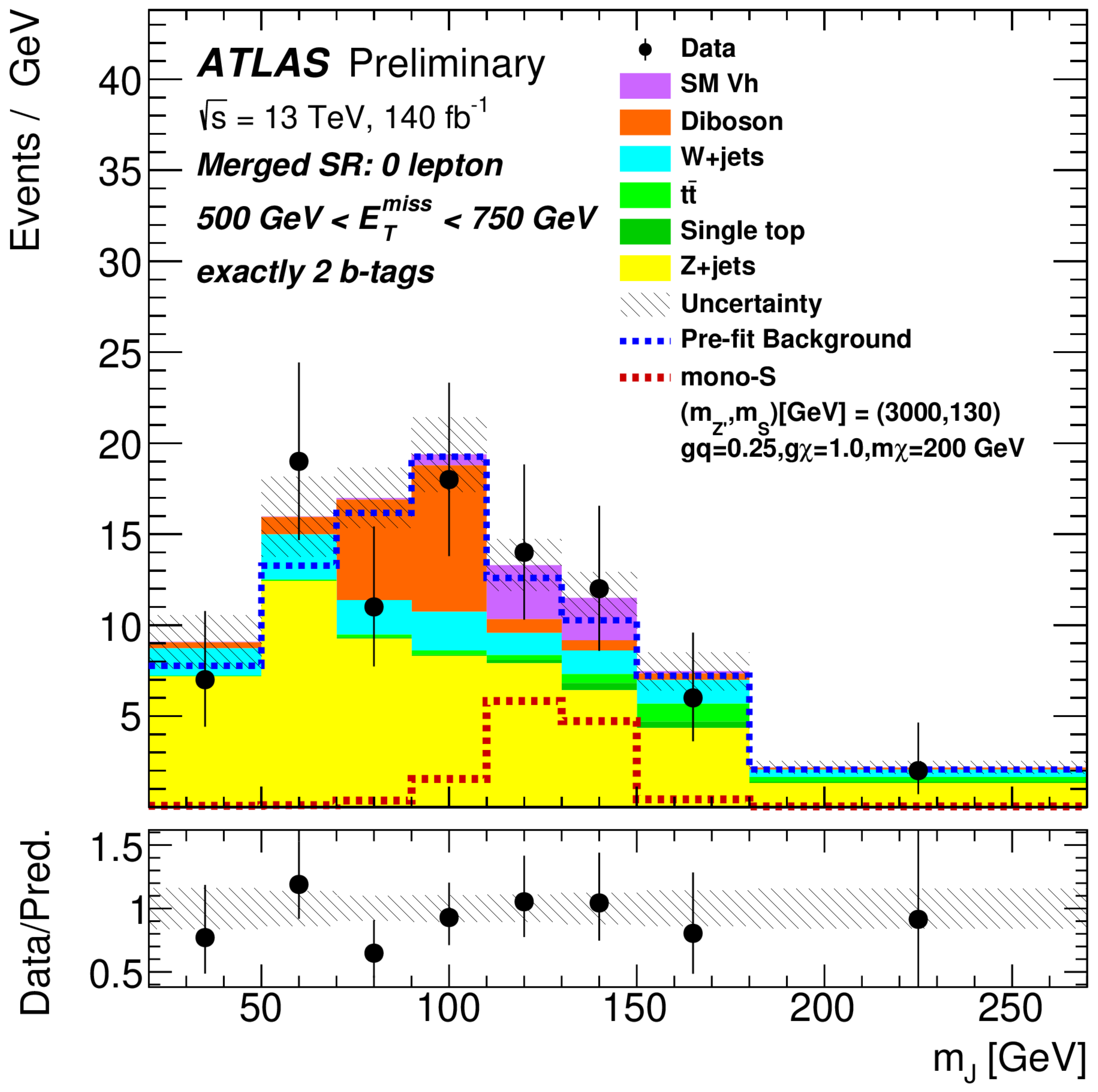

resolved

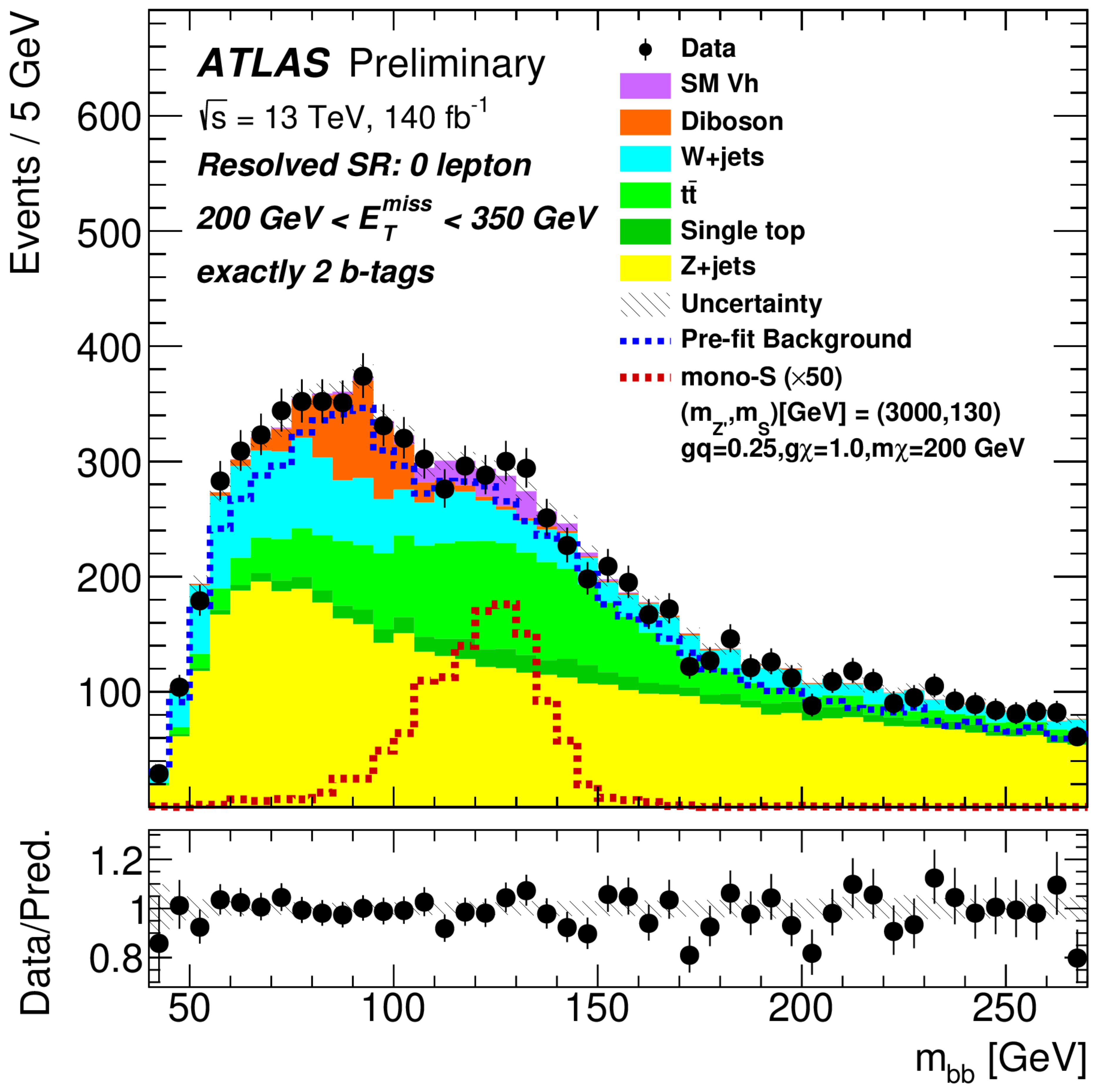

fit on m_J or m_{bb} shape in the SRs + yield in CRs simultaneously

Limit Contours in $m_{Z'}$-m_S-plane

- Xbb tagger can improve the limit results by up to 30%

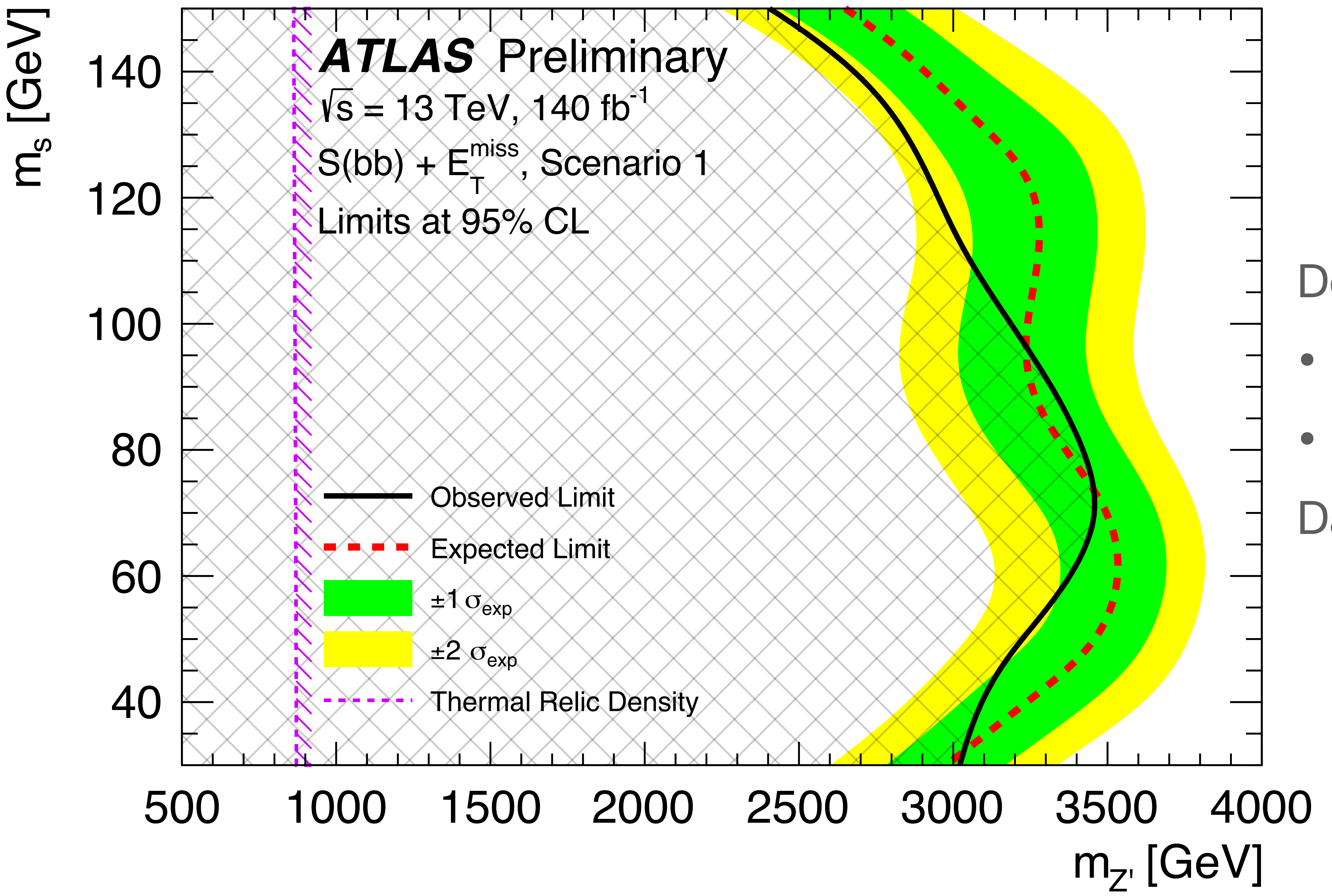

Dominant systematic uncertainties from:

- large-R jet b-tagging (Xbb tagger) calibration
- modeling of Z+jets

Data statistical uncertainties dominated.

Summary on Limit Contours

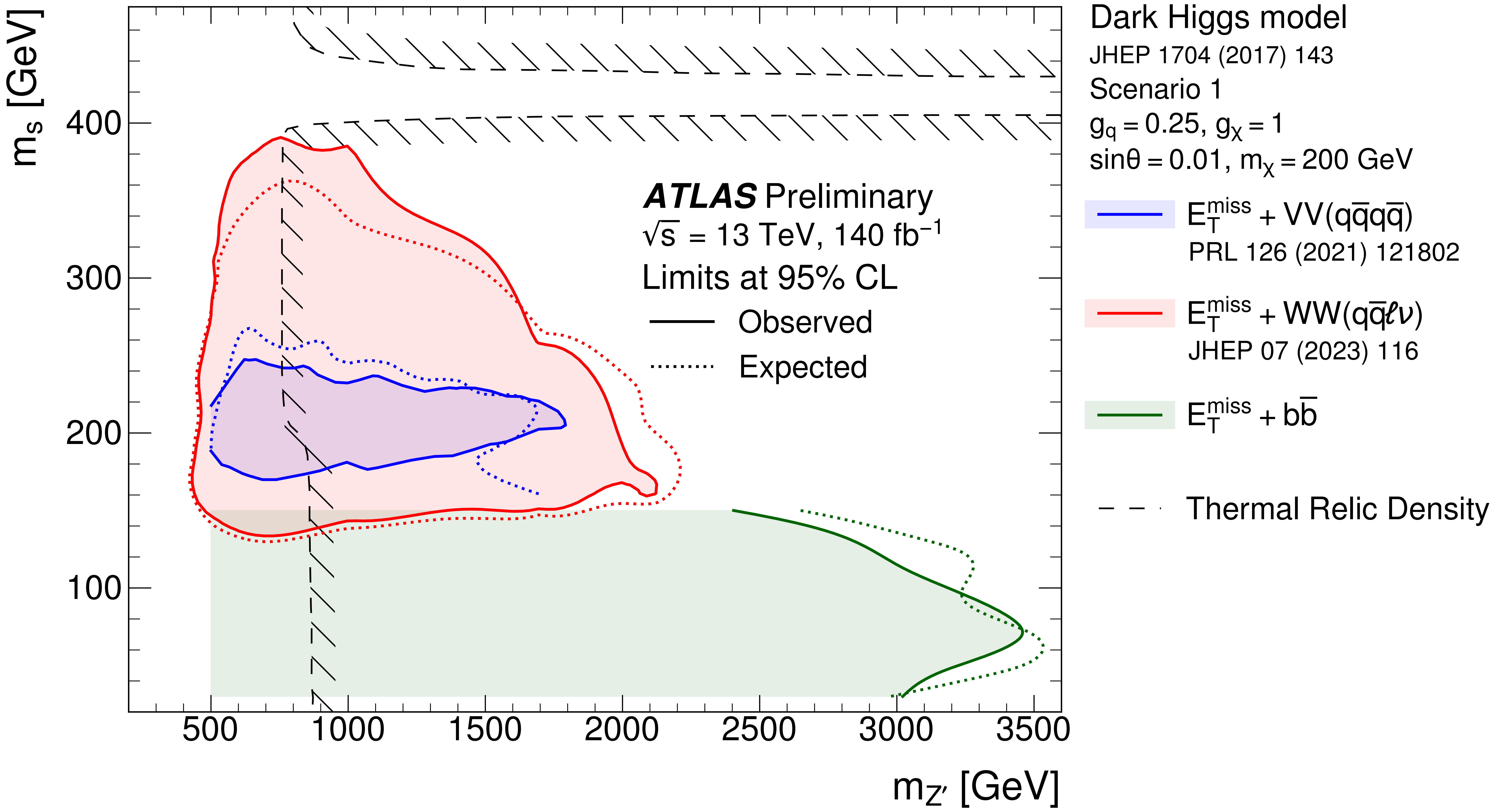

$m_s > 150$ GeV

Thanks to the cleaner signature in monoSWW semilep. has a stronger exclusion power than monoSVV had

$m_s \leq 150$ GeV

monoSbb has a strongest exclusion power at high $m_{Z'}$

Constraint from observed DM relic abundance

- Up to now fixing g_q = 0.25 and g_X = 1.0, this has important drawbacks when
  1. The couplings combination adopted so far is excluded by di-jet resonances for a wide range of Z' masses
  2. The observed DM relic abundance only reproduced for certain combination of the masses of the particles in the dark sector

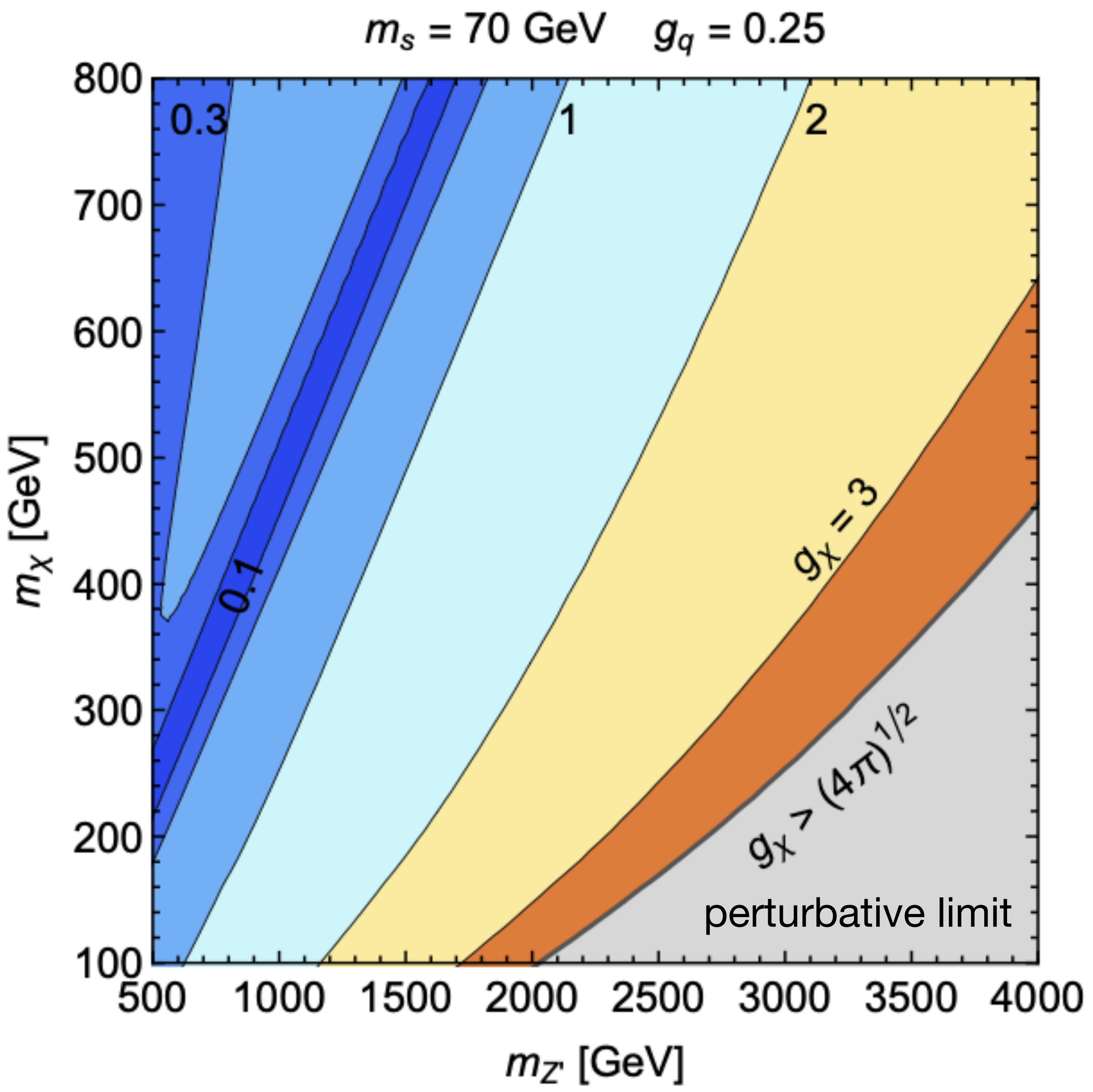

values of g_X determined by the relic abundance

When constraint from the observed DM relic abundance considered (fixing g_q), possible DM annihilation processes:

- XX → Z' → qq
  - when $m_X \approx m_{Z'}/2$, resonantly enhanced, dominant, small g_X is sufficient to reproduce relic abundance
- XX → ss → SM
  - becomes leading when far from $m_X \approx m_{Z'}/2$
- Larger Z'-DM coupling also implies a larger partial decay width for Z' →XX, di-jet signal rates suppressed

Two new scenarios proposed

	Parameters	m_S	Fixed values of the rest parameters
1	m_S - $m_{Z'}$	30 < m_S < 150 GeV	$\sin\theta$ = 0.01, m_χ = 200 GeV, g_q = 0.25, g_χ = 1.0
2	m_S - $m_{Z'}$	30 < m_S < 150 GeV	$\sin\theta$ = 0.01, m_χ = 900 GeV, g_q = 0.25, g_χ determined by relic density
3	m_χ - $m_{Z'}$	m_S = 70 GeV	$\sin\theta$ = 0.01, g_q = 0.25, g_χ determined by relic density

- In addition to the LHCDM WG recommendation, monoSbb analysis proposes:
  - Scenario2: gX = 1 → value determined by relic density abundance, m_χ increased to 900 GeV
  - Scenario3: gX = 1 → value determined by relic density abundance, m_S = 70 GeV for the largest sensitivity on m_χ - $m_{Z'}$ - plane, also proposed in paper JHEP 04 (2017) 143

Looking forward to further discussions

Limit Contours from monoSbb

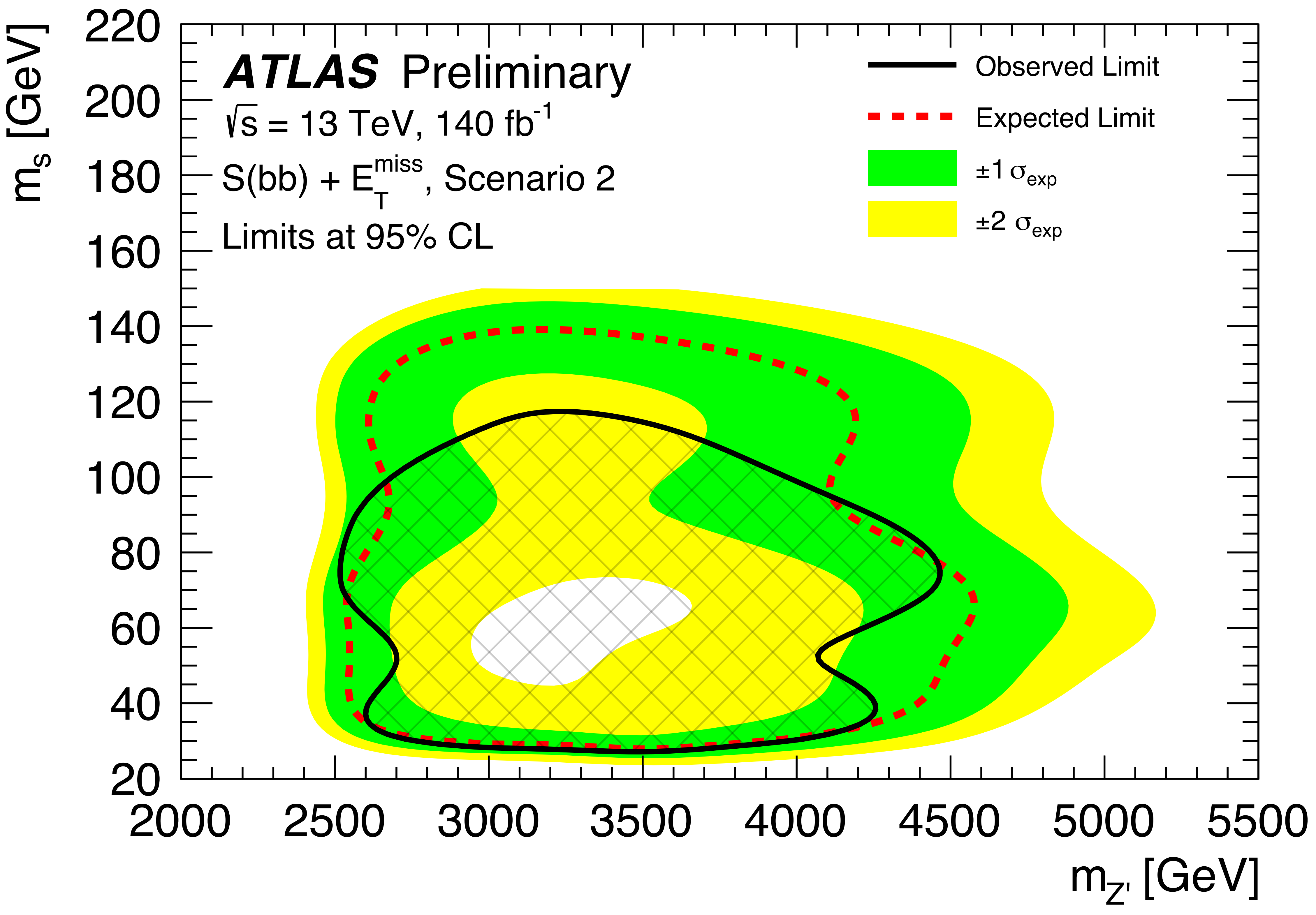

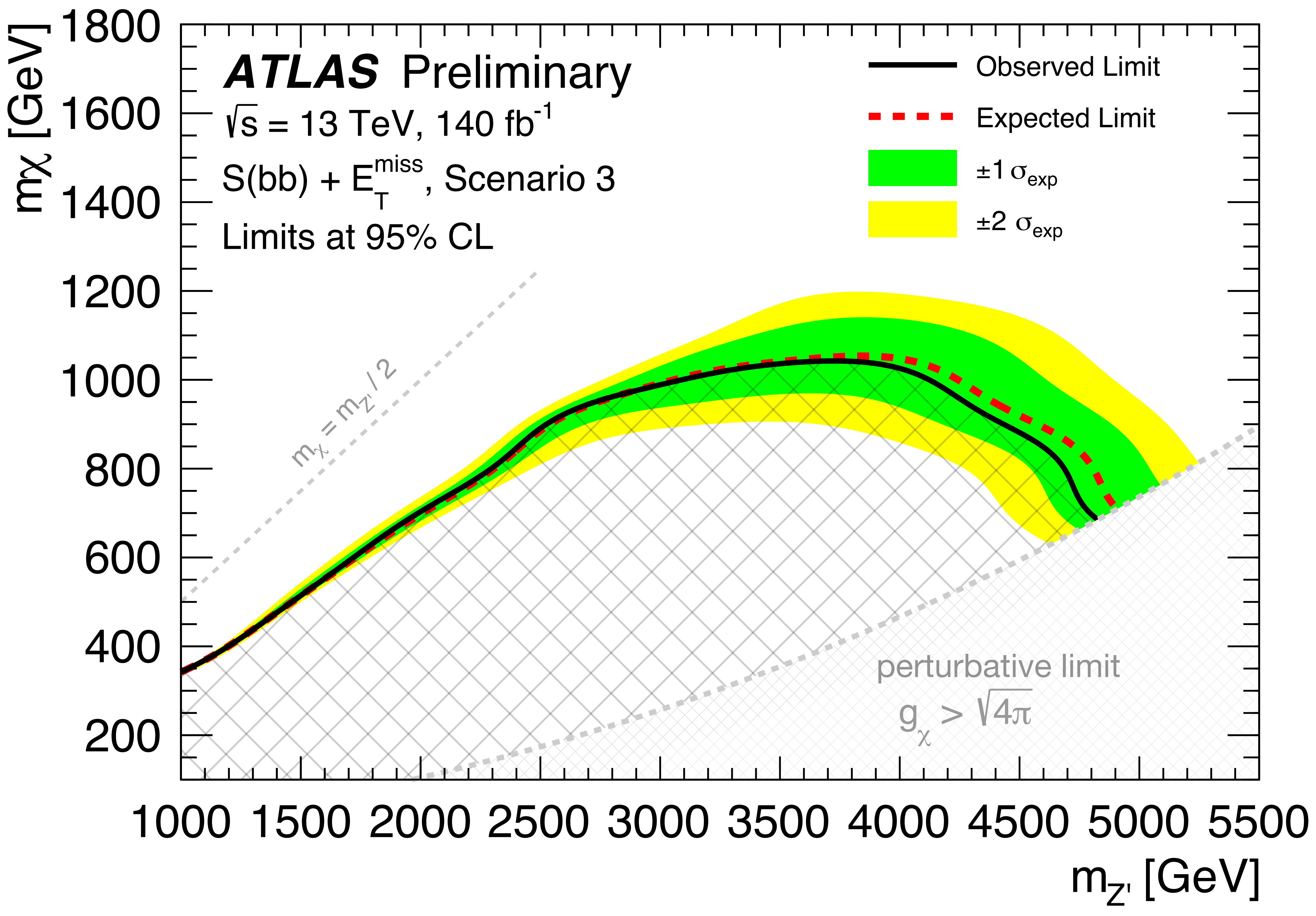

$\sin\theta = 0.01$, m_χ = 900 GeV, $g_q = 0.25$,

g_χ determined by relic density

m_S = 70 GeV, $\sin\theta = 0.01$, $g_q = 0.25$,

g_χ determined by relic density

Summary and Outlook for Run3

- Targeting 2MDM models, three analyses introduced
  - Thanks to the novel techniques, the sensitivities are enhanced and strong constraining power obtained
- Towards Run3, we will / may have:
  - large data statistics (a big benefit to monoSbb)
  - better background modeling (W/Z+jets)
  - new large-R jet reconstruction
    - with new dedicated tagger for W/Z in the dense environment to replace the TAR jet to simplified the signal reconstruction (benefit to monoSVV)
    - with new Xbb tagger (GN2x) (benefit to monoSbb)
  - other final states:
    - $s \to WW \to l\nu l\nu$, already done by CMS, see the next talk from Alicia Calderon Tazon
    - $s \to ZZ \to$ 4lep, clean signature though low branching ratio, maybe not practical yet
  - combination across two experiments

Backup

Feynman Diagram for monoSWW Production

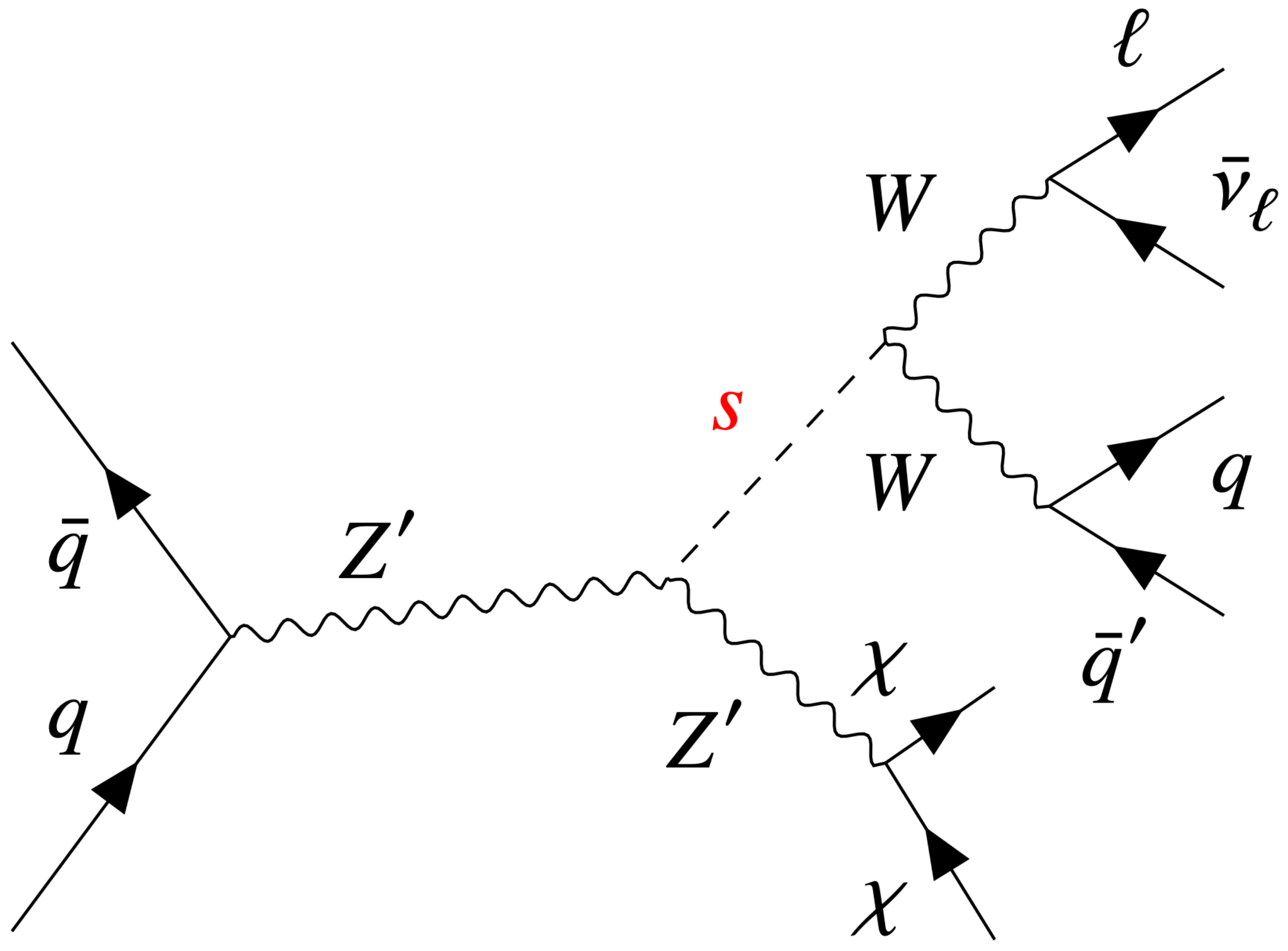

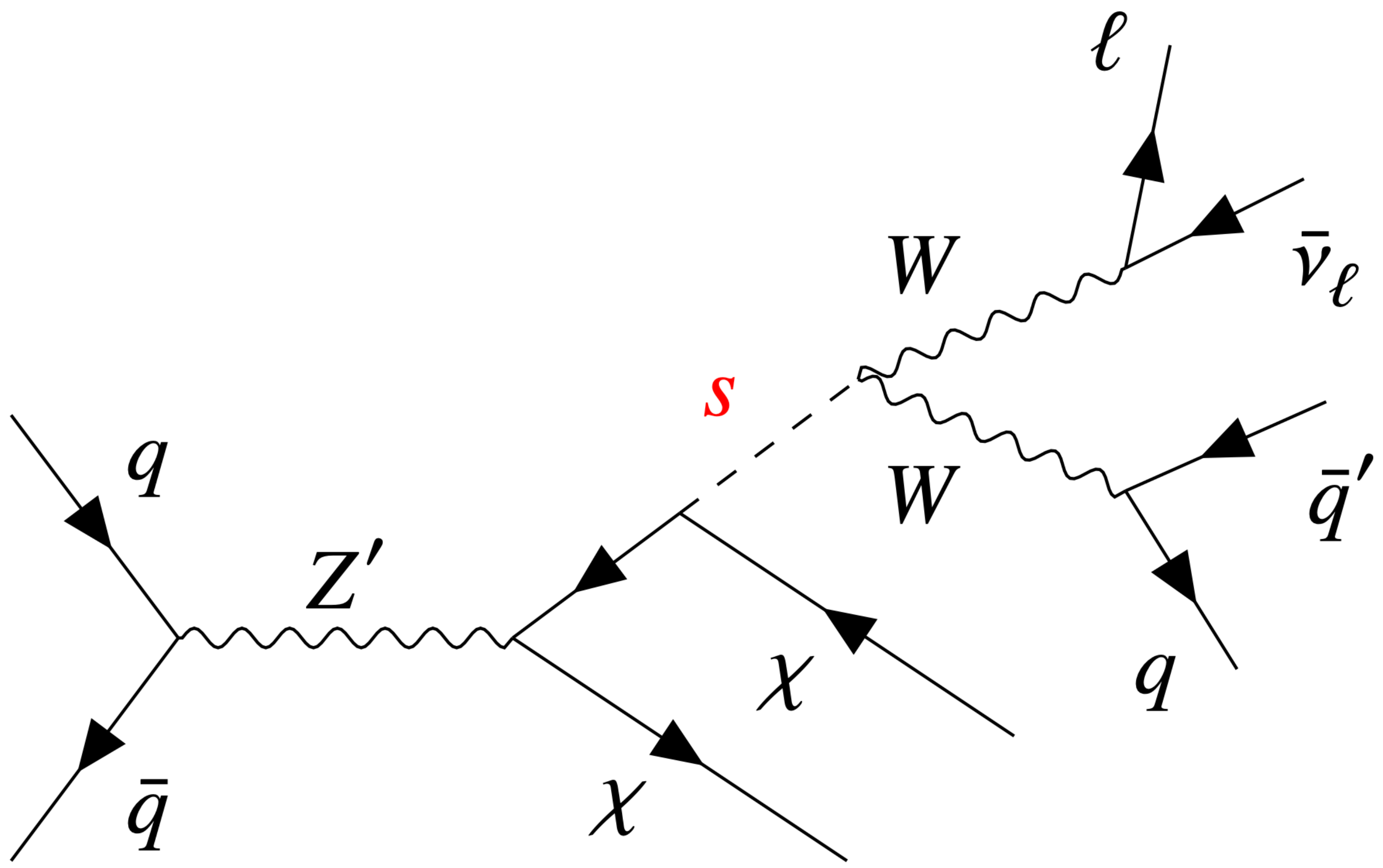

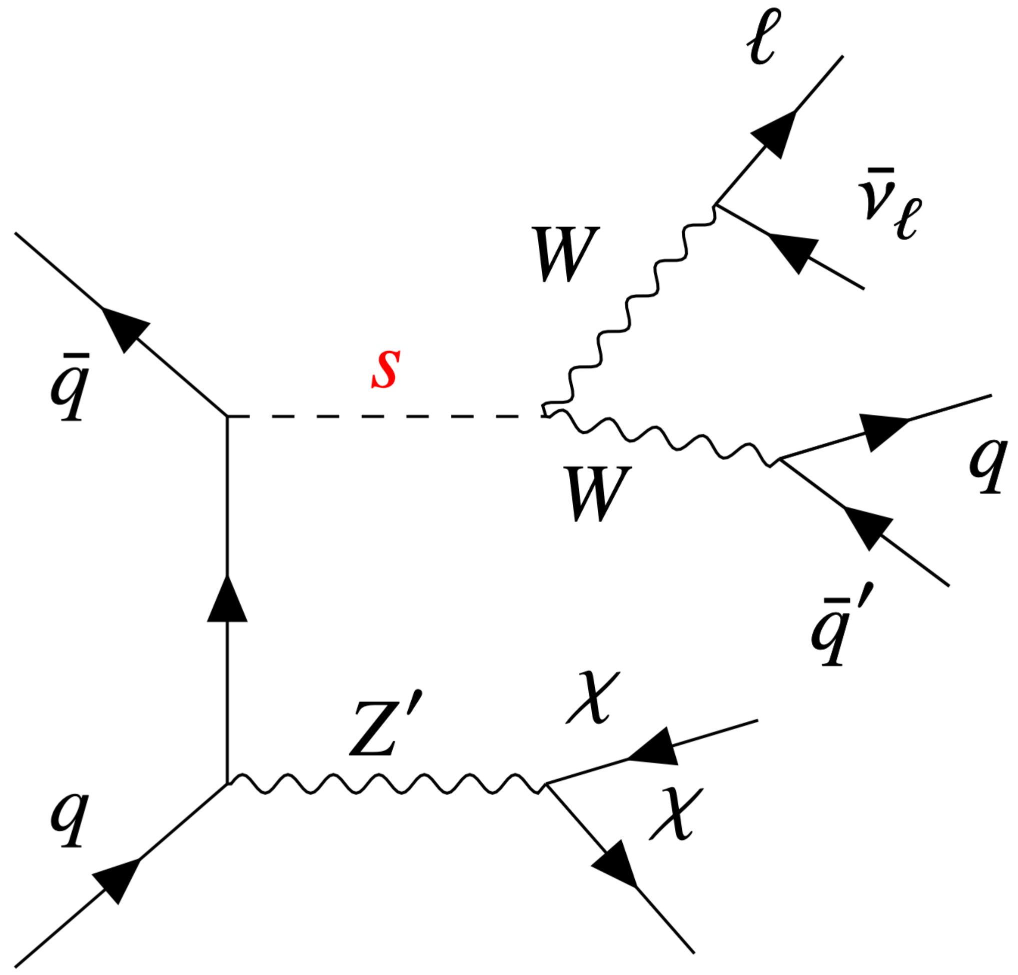

Typically dominates for high $m_{Z'}$

Sizable contribution throughout the parameter space considered

Contribution most for $m_{Z'} < 2m_\chi + m_S$

Reconstruction of TAR jets

- s to VV in Hadronic

scalar boson candidate mass: invariant mass of R=0.8 TAR jet with highest pt

Track-Assisted Reclustered jet: jet re-clustering algorithm using AntiKt4EMTopoJets with substructure information computed from tracks matched to the constituent jets

Track quality selection	Loose
Track p_T	> 0.5 GeV
Track $\|\eta\|$	< 2.5
Track Si hits	7 or more
Track to vertex association: $z_0 \times \sin(\theta)$	< 3.0 mm
Track to vertex association: transverse distance d_0	< 2.0 mm
Input jet selection	signal $R = 0.4$ jets
Input jet p_T	$p_T^{jet} > 20$ GeV
Reclustering radius	$R = 0.8$
TAR jet p_T	$p_T^{TAR} > 100$ GeV
Trimming radius	$R = 0.2$
Trimming p_T fraction	0.05
Track to jet association	$\Delta R(\text{jet, track}) < 0.5$

- s to WW in Leptonic

- track-assisted reclustering, using tracks and calibrated R=0.2 LCW (R-scan) jets as input
- lepton disentanglement: remove tracks associated with electrons/mouns, and R=0.2 jets within ΔR<0.2 of an electron from input
- jets are reclustered with R=1 AntiKt
- tracks are associated to R=0.2 jets and rescaled to jet p_T
- mass and substructure of TAR jets are calculated from tracks, making use of superior tracking resolution

Track selection	Loose quality $p_T > 0.5$ GeV $\|\eta\| < 2.5$
Track-to-vertex association	$\|z_0 \times \sin\theta\| < 3.0$ mm $\|d_0\| < 2.0$ mm
Tracks removed if associated to	electrons, muons
Input jet selection	$R = 0.2$ topo jets $p_T > 20$ GeV $\|\eta\| < 2.5$
Reclustering radius	$R = 1.0$
TAR jet p_T	$p_T^{TAR} > 100$ GeV
Trimming radius	$R = 0.2$
Trimming p_T fraction	$f_{cut} = 0.05$
Track-to-jet association	$\Delta R(\text{jet, track}) < 0.3$
jet-electron overlap removal	$\Delta R(\text{jet, electron}) < 0.2$

Jet substructure / shape variables

- Energy Correlation ratios, C2 and D2

$$\mathrm{ECF1} = \sum_{i \in J} p_{\mathrm{T}_i},$$

$$\mathrm{ECF2}(\beta^{\mathrm{ECF}}) = \sum_{i<j \in J} p_{\mathrm{T}_i} p_{\mathrm{T}_j} \left(\Delta R_{ij}\right)^{\beta^{\mathrm{ECF}}},$$

$$\mathrm{ECF3}(\beta^{\mathrm{ECF}}) = \sum_{i<j<k \in J} p_{\mathrm{T}_i} p_{\mathrm{T}_j} p_{\mathrm{T}_k} \left(\Delta R_{ij} \Delta R_{ik} \Delta R_{jk}\right)^{\beta^{\mathrm{ECF}}},$$

$$e_2 = \frac{\mathrm{ECF2}}{(\mathrm{ECF1})^2}, \qquad C_2 = \frac{e_3}{(e_2)^2},$$

$$e_3 = \frac{\mathrm{ECF3}}{(\mathrm{ECF1})^3}. \qquad D_2 = \frac{e_3}{(e_2)^3}.$$

- N-subjettiness ratios $\tau_{21} = \frac{\tau_2}{\tau_1}$ and $\tau_{32} = \frac{\tau_3}{\tau_2}$ (used to distinguish W and top jets)

$$\tau_0(\beta^{\mathrm{NS}}) = \sum_{i \in J} p_{\mathrm{T}_i} R_0^{\beta^{\mathrm{NS}}},$$

$$\tau_1(\beta^{\mathrm{NS}}) = \frac{1}{\tau_0(\beta^{\mathrm{NS}})} \sum_{i \in J} p_{\mathrm{T}_i} \Delta R_{a_1,i}^{\beta^{\mathrm{NS}}},$$

$$\tau_2(\beta^{\mathrm{NS}}) = \frac{1}{\tau_0(\beta^{\mathrm{NS}})} \sum_{i \in J} p_{\mathrm{T}_i} \min(\Delta R_{a_1,i}^{\beta^{\mathrm{NS}}}, \Delta R_{a_2,i}^{\beta^{\mathrm{NS}}}),$$

$$\tau_3(\beta^{\mathrm{NS}}) = \frac{1}{\tau_0(\beta^{\mathrm{NS}})} \sum_{i \in J} p_{\mathrm{T}_i} \min(\Delta R_{a_1,i}^{\beta^{\mathrm{NS}}}, \Delta R_{a_2,i}^{\beta^{\mathrm{NS}}} \Delta R_{a_3,i}^{\beta^{\mathrm{NS}}}),$$

Analytical solution of s→WW→qqlv system

$$E_\nu = \frac{m_W^2}{2E_\ell(1-\cos\theta_{\ell\nu})}$$

$$p_\nu = \frac{m_W^2}{2E_\ell(1-\cos\theta_{\ell\nu})}(\sin\theta_{\ell\nu}\cos\phi_\nu, \sin\theta_{\ell\nu}\sin\phi_\nu, \cos\theta_{\ell\nu}, 1)$$

The invariant mass of the $s \to WW$ system is then

$$\begin{aligned} m_s^2 = & \ (p_{W_{\text{cand}}} + p_\ell + p_\nu)^2 \\ = & \ (E_{W_{\text{cand}}} + E_\ell + E_\nu)^2 - (p_{x,W_{\text{cand}}} + E_\nu \sin\theta_{\ell\nu}\cos\phi_\nu)^2 \\ & - (E_\nu \sin\theta_{\ell\nu}\sin\phi_\nu)^2 - (E_\ell + p_{z,W_{\text{cand}}} + E_\nu\cos\theta_{\ell\nu})^2 \end{aligned}$$

It can be shown that the minimum occurs when $\phi_\nu = 0$.

$$m_s^2 = \left(E_\ell + \frac{m_W^2}{2E_\ell(1-\cos\theta_{\ell\nu})} + E_{W_{\text{cand}}}\right)^2 - \left(\left|\vec{p}_{W_{\text{cand}}}\right| \sin\theta_{W_{\text{cand}}\ell} + \frac{m_W^2\sqrt{1-\cos^2\theta_{\ell\nu}}}{2E_\ell(1-\cos\theta_{\ell\nu})}\right)^2 - \left(E_\ell + \left|\vec{p}_{W_{\text{cand}}}\right|\cos\theta_{W_{\text{cand}}\ell} + \frac{m_W^2\cos\theta_{\ell\nu}}{2E_\ell(1-\cos\theta_{\ell\nu})}\right)^2,$$

leaves only $\cos\theta_{\ell\nu}$ as an unknown

$$m_s^{\min} \equiv \min_{\cos\theta_{\ell\nu}}(m_s)$$

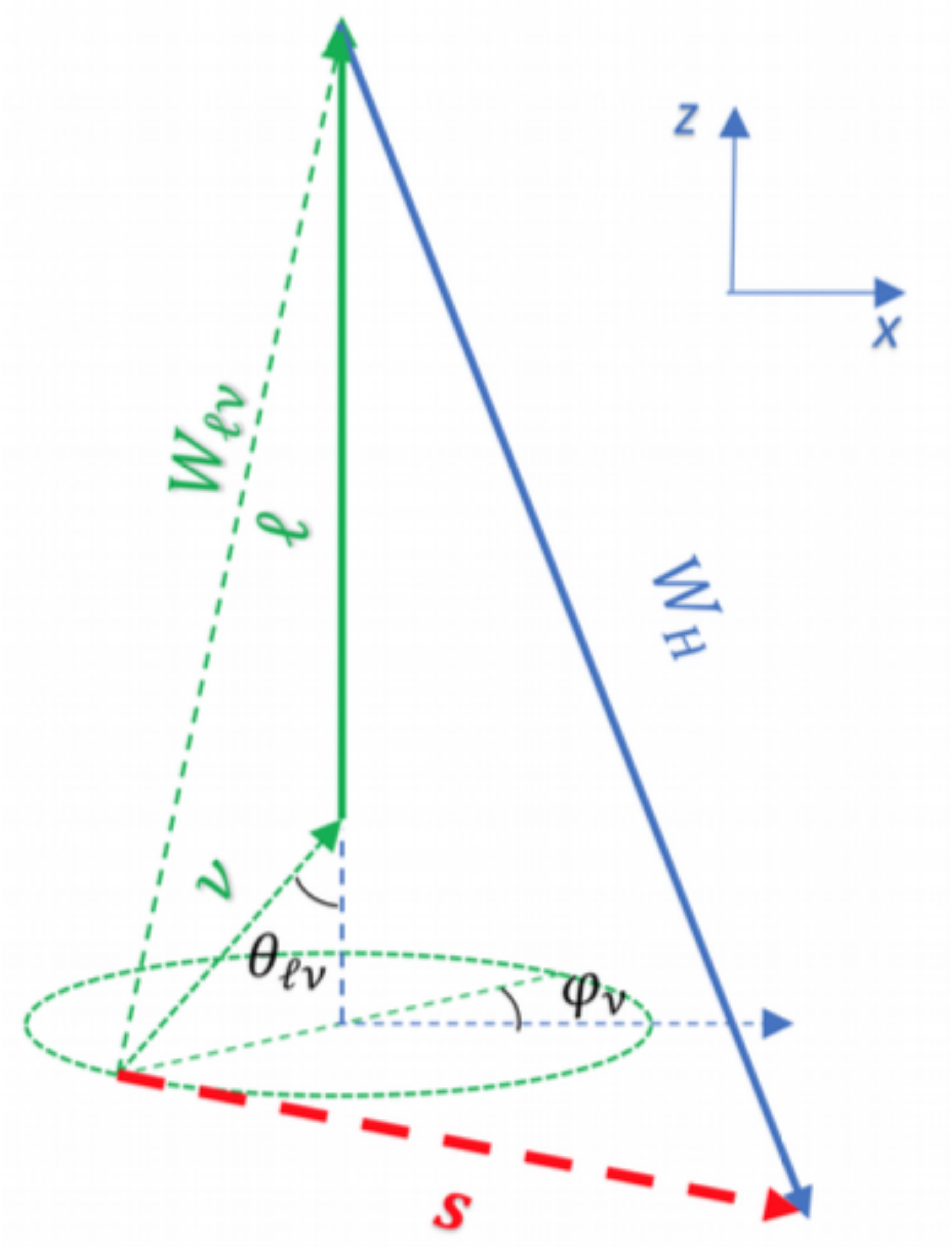

Reconstruction of TAR jets